CHAPTER IV

RESULTS AND DISCUSSION

4.1 Determination of TCs using an anodized BDD electrode

This study focused on the method development of the tetracycline antibiotic determination, based on the electrochemical method using an anodized BDD electrode. The study was separated into 3 parts including cyclic voltammetry, flow injection, and HPLC with amperometric detection. The details of each part were described as the follows.

4.1.1 Investigation of TCs using cyclic voltammetry

4.1.1.1 Voltammetric study of TCs

As commonly known, the synthesis of as-deposited BDD electrodes by microwave plasma-assisted chemical vapor deposition is hydrogen-terminated on the diamond surface. The chemical modification can be carried out by anodic polarization or oxygen plasma treatment to change the hydrogen-terminated surface to an oxygen-terminated surface one. In this study, anodic polarization in alkaline solution (0.1 M potassium hydroxide) was used, as described in the experiment chapter. The major type of oxygen functional group is the carbonyl group, which is believed to exist on (100) faces. The highly oriented carbonyl groups provide a surface dipolar field that could repel a neutral molecule with oxygen-containing functional groups surrounding a central core. On the other hand, the oxygen plasma treatment or thermal oxidation can induce the bridge form of C-O-C on the surface of diamond [81].

The electrooxidation of four TCs was investigated on as-deposited BDD, GC, and anodized BDD electrodes. Figures 4.1-4.4 show cyclic voltammograms of 500 μM of TCs in 0.1 potassium dihydrogen phosphate (pH 2) together with the background voltammograms at the as-deposited BDD, GC, and anodized BDD electrodes. All electrodes provided irreversible cyclic voltammograms.

This irreversible behavior suggested that TCs were oxidized, and then reacted rapidly to form a new product. Cyclic voltammetric results of TC, CTC, OTC, and DC at as-deposited BDD, GC, and anodized BDD electrodes are summarized in Table 4.2. Results showed that the highest current signals were obtained for TC, CTC, OTC, and DC at the anodized BDD electrode and they can be explained in recent work carried out with glutathione [82] on the basis of attractive electrostatic interaction between the negatively charged anodized surface and the positively charged substrates. TCs were fully positively charged in strongly acidic pH, as we used in this experiment. Hence, the positively charged substrates could be attracted to the negative surface of the anodized BDD electrode, which induced the electrooxidation to occur easily. In contrast to as-deposited BDD, the surface is positively charged and non-polar (covered with hydrogen atoms), and the electrostatic interaction was less permitted, which presumably resulted in the ill-defined cyclic voltammagrams.

Table 4.1 Electrochemical oxidation data obtained from cyclic voltammetry of OTC, TC, CTC, and DC at as-deposited BDD, GC, and anodized BDD electrodes.

Analytes	Concentration	As-deposited BDD		GC		Anodized BDD	
	(μM)	E_p (V)	i_p (μA)	E_p (V)	i_p (μA)	E_p (V)	i_p (μA)
OTC	100	1.12	1.21	1.08	2.05	1.59	5.03
	500	1.13	2.02	1.09	6.51	1.69	32.34
TC	100	1.14	1.16	1.08	2.65	1.54	5.20
	500	1.16	3.22	1.06	8.85	1.65	29.88
CTC	100	1.06	1.03	0.99	1.59	1.57	4.67
	500	1.10	3.67	1.02	6.44	1.63	26.10
DC	100	1.04	1.06	0.99	2.95	1.56	4.85
	500	1.07	4.01	1.00	7.77	1.66	28.70

The scan rate dependence study was carried out by a variation of scan rate range from 10 to 300 mv s^{-1}. The equations used for describing the relationship between the current signal and scan rate in the case of the analyte undergoing irreversible reaction are shown below [110]:

$$i_p \text{ (diffusion)} = (2.99 \times 10^5) n(\alpha n_a)^{1/2} A\, C_0^{*}\, D_0^{1/2} \nu^{1/2} \text{ ----------4.1}$$

$$i_p \text{ (adsorption)} = n\alpha n F^2 A \nu \Gamma^{*}_0 / 2.718RT\text{----------4.2}$$

From equation 4.1 and 4.2, the current (diffusion) is expected to be proportional to the square root of scan rate, $\nu^{1/2}$ while the current (adsorption) is expected to be proportional to the scan rate, ν . At the anodized diamond electrode, the relationship between the current and the square root of the scan rate was linear with a correlation coefficient of 0.99. Therefore, it can be concluded that tetracycline underwent irreversible reaction and also semi-infinite linear diffusion of reactant to the anodized diamond electrode surface.

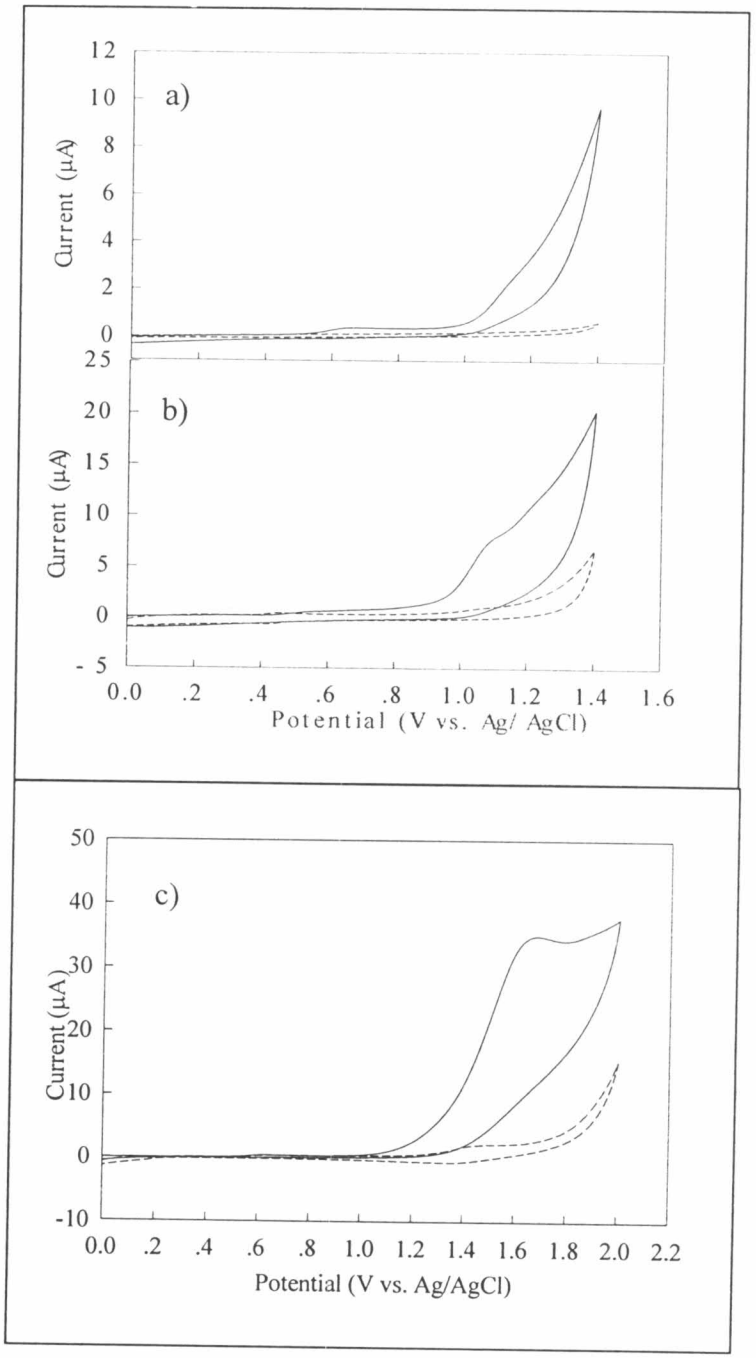

Figure 4.1 Cyclic voltammograms of 500 μM OTC (solid line) in 0.1 M potassium hydrogen phosphate (pH 2) together with the corresponding background current (dashed line) at a) as-deposited BDD b) GC, and c) anodized BDD electrodes.

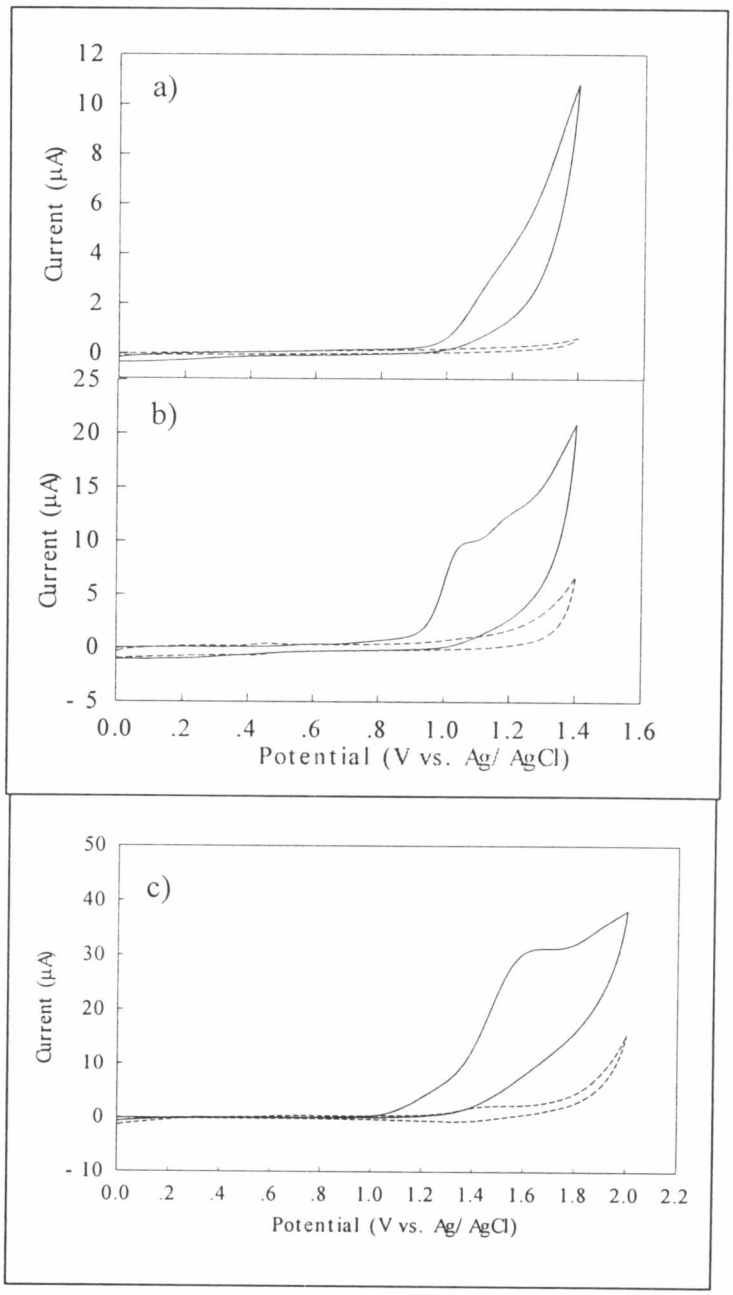

Figure 4.2 Cyclic voltammograms of 500 μM TC (solid line) in 0.1 M potassium dihydrogen phosphate (pH 2) together with the corresponding background current (dashed line) at a) as-deposited BDD b) GC, and c) anodized BDD electrodes.

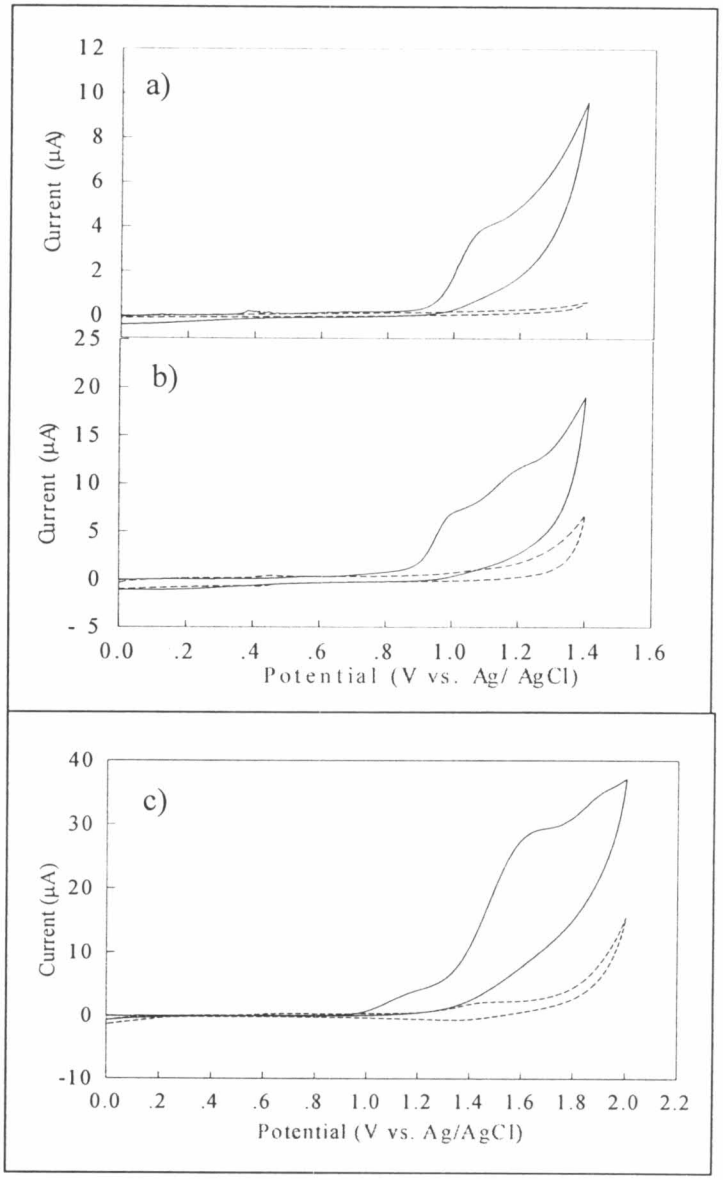

Figure 4.3 Cyclic voltammograms of 500 μM CTC (solid line) in 0.1 M potassium dihydrogen phosphate (pH 2) together with the corresponding background current (dashed line) at a) as-deposited BDD b) GC, and c) anodized BDD electrodes.

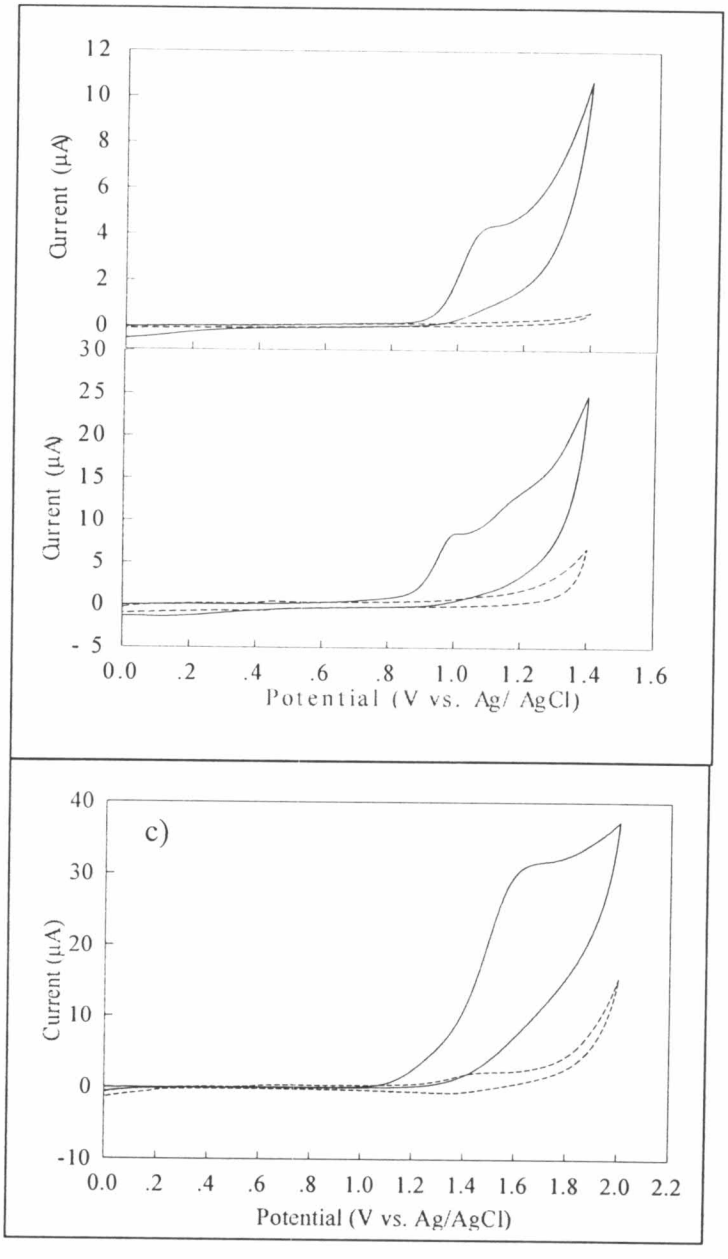

Figure 4.4 Cyclic voltammograms of 500 μM DC (solid line) in 0.1 M potassium dihydrogen phosphate (pH 2) together with the corresponding background current (dashed line) at a) as-deposited BDD b) GC, and c) anodized BDD electrodes.

4.1.1.2 pH dependence

To find the optimum pH for detection of four TCs, the experiments were carried in the pH solution ranged from 2 to 9 at anodized BDD electrode. A plot of pH versus E_p was investigated (Fig. 4.5) with ambiguous results and the expected pK_a was inconsistent with the pK_a value of the dissociation in the literature.

The details concerning the current response and peak potential of TCs at each pH was investigated, as shown in Table 4.2. In acidic buffer, the well-resolved cyclic voltammograms of tetracyclines were obtained whereas, in neutral and alkaline buffer, ill-defined cyclic voltammograms were obtained. Results for all TCs demonstrated that pH 2 gave the highest current signal.

It can be explained that tetracyclines are derived from a system of four membered rings arranged linearly with characteristic double bonds. They are amphoteric compounds with high polarity and an isoelectric point between 4 and 6. From the reference literature, three portotropic dissociations have been observed for TCs, with pK_1, pK_2, and pK_3 as shown in Table 4.3. In strongly acidic pH, the tetracycline molecules exist as fully protonated from as a singly charged cation. As proposed in the previous work [4,82], the surface of anodized BDD is negatively charged, and the electrostatic interaction between the negatively charged covering of the anodized surface and the positively charged substrates is attractive. Hence, the fully positively charged TCs at pH 2 provided the highest response, and this pH was chosen as the optimum pH for the rest of the experiments.

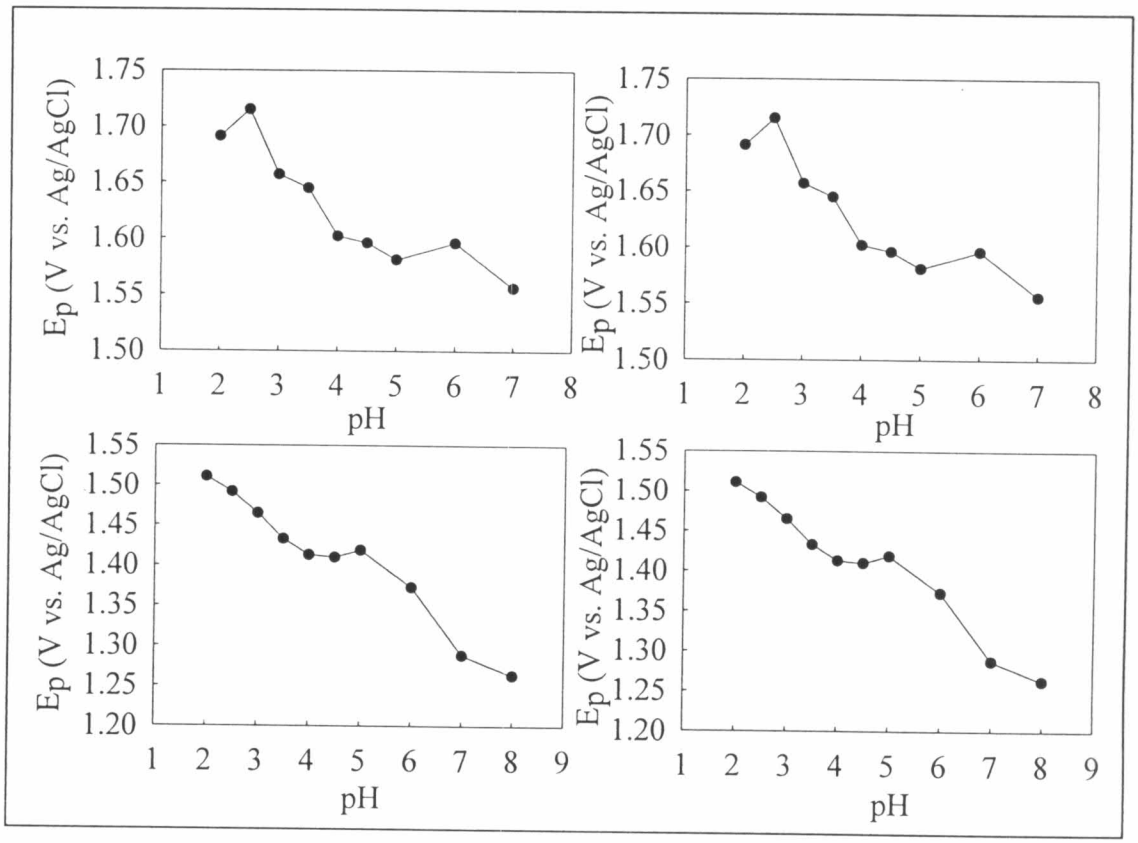

Figure 4.5 Relationship between the pH and E_p.

Table 4.2 Electrochemical oxidation data obtained from cyclic voltammetry of 1 mM OTC, TC, CTC, and DC at anodized BDD electrodes.

pH	OTC		TC		CTC		DC	
	E_p (V)	i_p (μA)	E_p (V)	i_p (μA)	E_p (V)	i_p (μA)	E_p (V)	i_p (μA)
2	**1.65**	**170.20**	**1.69**	**161.80**	**1.54**	**242.90**	**1.51**	**191.30**
2.5	1.65	146.60	1.72	130.80	1.57	178.40	1.49	161.50
3	1.61	130.20	1.66	127.80	1.55	173.30	1.47	156.40
3.5	1.60	138.70	1.65	132.50	1.48	154.80	1.43	152.30
4	1.58	142.60	1.60	128.30	1.46	158.70	1.41	155.70
4.5	1.59	138.60	1.60	137.90	1.47	154.10	1.41	149.40
5	1.57	140.80	1.58	137.70	1.46	151.60	1.42	149.00
6	1.58	165.90	1.60	151.60	1.49	178.40	1.37	159.80
7	1.56	163.70	1.56	156.10	1.48	193.50	1.29	169.80
8		-		-	1.38	235.80	1.26	187.60
9		-		-		-		-

Table 4.3 pK_a values of TCs in aqueous solutions [111].

Analytes	pK_1	pK_2	pK_3
OTC	3.27	7.32	9.11
TC	3.30	7.68	9.69
CTC	3.30	7.68	9.27
DC	nf*	nf*	nf*

*nf : no reference found

4.1.2 Determination of TCs using flow injection with amperometric detection

4.1.2.1 Hydrodynamic voltammetry

To find the optimum potential, hydrodyanamic voltammetry was carried out. A hydrodynamic voltammogram was obtained from the average of three aliquot injections of the 20 μL of 100 μM TCs solutions in the flow injection system at increasing values of the applied potential from 1.1 to 2.0 V vs. Ag/AgCl in the flow injection system. The carrier solution was 0.1 M potassium dihydrogen phosphate (pH 2). Fig 4.6a shows the hydrodynamic voltammogram of TCs with the corresponding background current. The hydrodynamic voltammogram of TCs did not exhibit the sigmodial shape of the signal vs. potential probably due to the high oxidation potential of TCs. To obtain the optimum potential, the S/B ratios from Fig 4.6b were calculated at each potential and plot the results versus the potential. The maximum S/B ratio was found at 1.5 V. vs. Ag/AgCl for CTC and 1.6 V vs. Ag/AgCl for TC, OTC, and DC. Hence, this study used these optimum potentials for the quantification experiment in the flow injection system.

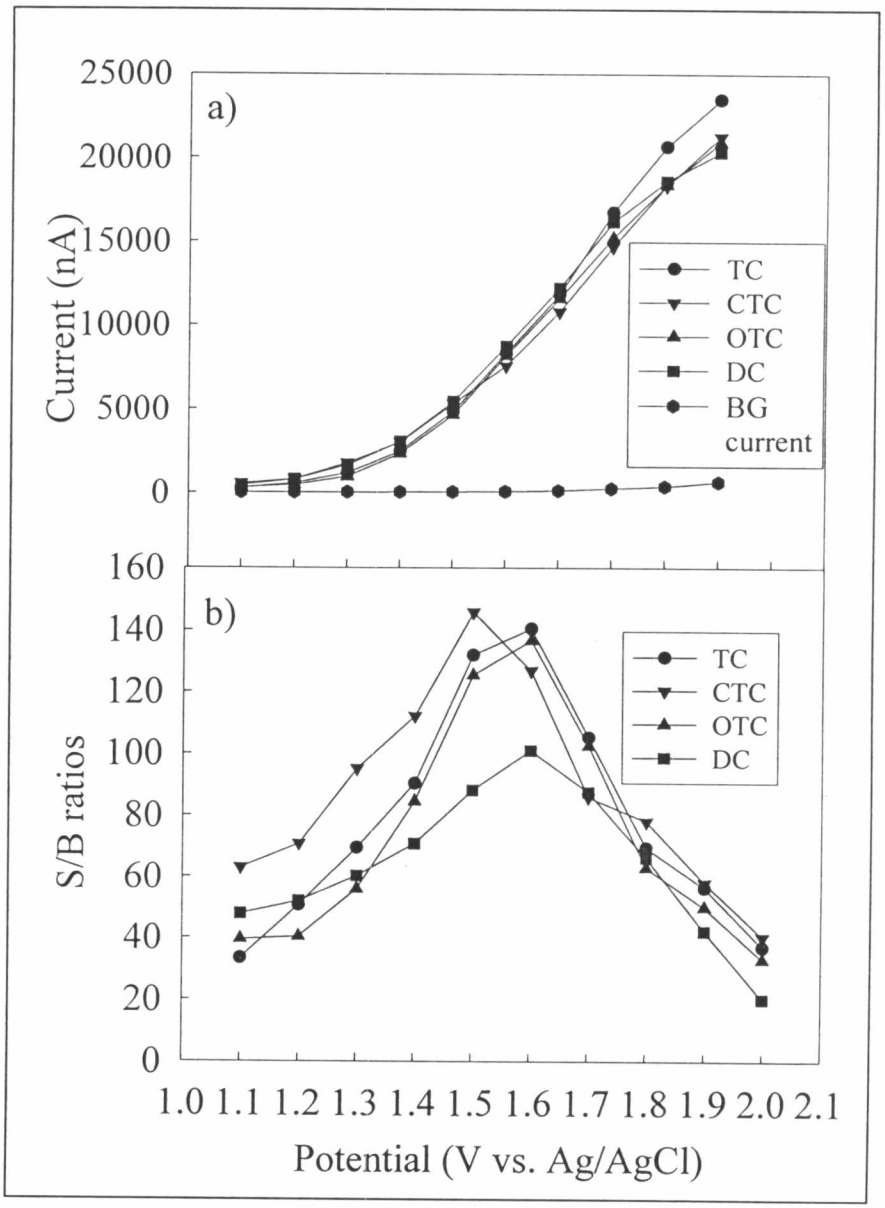

Figure 4.6 a) Hydrodynamic voltammogram for 100 μM TCs (●) : OTC; (▲):TC; (▼): CTC; and (■):DC in 0.1 M potassium dihydrogen phosphate (pH 2), using 0.1 M potassium dihydrogen phosphate (pH 2) as carrier solution. The flow rate was 1 mL min^{-1}. b) Hydrodynamic voltammogram of signal-to-background ratios.

4.1.2.2 Analytical performance of anodized BDD electrode using the flow injection system

A series of analytical figures of merit were performed on the proposed method for the quantification of TC, CTC, OTC, and DC.

Linearity and LOD: the calibration curves were constructed separately for each drug in the concentration range of 0.1 to 1000 μM as shown in Fig. 4.7. Each point of the calibration graph corresponded to the mean value from three replicated injections. The regression analysis parameters for each TC standard solution were summarized such as the linear range and LOD in Table 4.4. Linear range of the method was about two orders of magnitude range from 0.1-50 for TC and 0.5-50 μM for OTC, CTC, and DC. The LOD defined as the concentration that provided the signal-to-noise ratio of 3 was 10 nM for the four TCs.

Repeatability: to check the repeatability of the proposed method, the experiments were carried out by injecting 10 replicates of the three concentrations (5, 10, 50 μM) of each drug. The peak variability defined as the relative standard deviation (%RSD) was 1.3-1.7, 2.4-3.0, 1.6-3.0, and 1.7-2.7 for TC, CTC, OTC, and DC, respectively.

Stability: the response received from anodized BDD electrodes with amperometric detection was very stable. The flow injection signal obtained by repetitive 100 injections of 50 μM CTC on the anodized diamond provided a peak variation of about 3.4%. Moreover, the anodized BDD electrode could be reactivated in situ by applying a high positive potential (2.6 V vs. Ag/AgCl) during the flow injection measurement. The sample throughput was approximately seventy injections per hour.

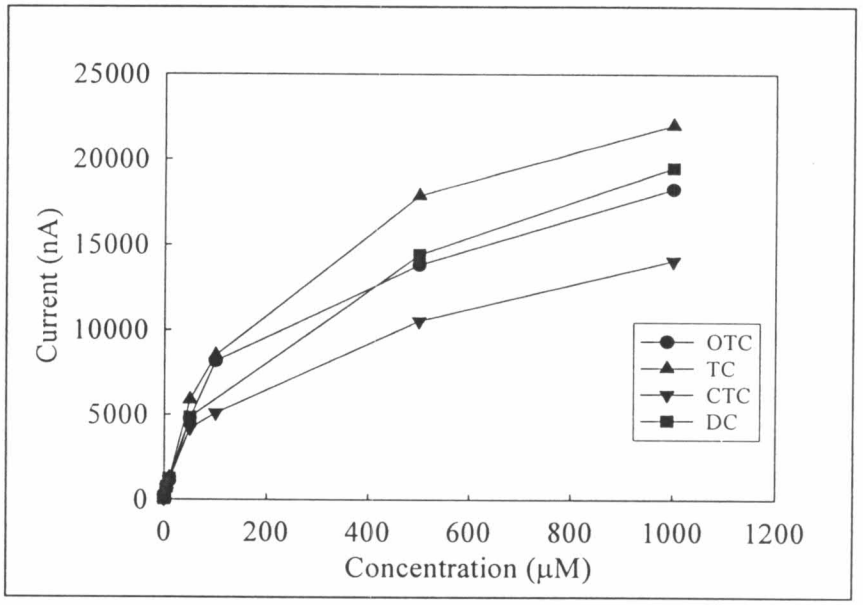

Figure 4.7 Calibration curves of four TCs (OTC, TC, CTC, and DC) using flow injection system.

Table 4.4 Regression analysis of[a] parameters, linear range, and LOD for the determination of TCs by FIA with amperometric detection using an anodized BDD electrode (n=2).

Analytes	Linear range (μM)	a	b	r^2	LOD (nM)
TC	0.1-50	110.00±5.96	192.13±4.86	0.9968±0.0006	10
CTC	0.5-50	76.93±3.87	199.72±29.68	0.9969±0.0001	10
OTC	0.5-50	90.23±2.99	165.17±28.86	0.9992±0.0006	10
DC	0.5-50	96.23±3.81	213.73±48.92	0.9966±0.0001	10

[a] y = ax+b, where y = current (nA), x = concentration (μM), a = slope (nA μM^{-1})

4.1.2.3 Application

The proposed method of this study was applied for drug formulations using the standard addition method. The precision of this method was based on the intra-assay and inter-assay. The amounts of each drug were compared with the label contents. The results are summarized in Table 4.5. There was no significant difference in results between the label contents and those obtained by the proposed method for the intra-assay and inter-assay precision (3 days). To check the accuracy of the method, recoveries of the spiked standard solution were evaluated. The results are summarized in Table 4.6.

Table 4.5 Results of TC determination in drug formulations.

Analytes	Intra-assay (n = 2)			Inter-assay (n = 6)		
	Label amount (mg)	Found (mg)	%Found	Label amount (mg)	Found (mg)	%Found
TC	250	249.4±1.7	99.8±0.7	250	246.3±3.2	98.5±1.3
CTC	250	249.7±1.3	99.9±0.5	250	247.3±4.0	98.9±1.6
OTC	250	254.6±2.5	101.9±1.0	250	257.5±3.3	103.0±1.3
DC	100	98.4±1.0	98.4±1.0	100	99.5±1.3	99.5±1.3

Table 4.6 Recovery studies for the determination of TCs in drug formulations.

Analytes	Intra-assay (n = 2)			Inter-assay (n = 6)		
	Added ($\mu g\ mL^{-1}$)	Found ($\mu g\ mL^{-1}$)	%Recovery	Added ($\mu g\ mL^{-1}$)	Found ($\mu g\ mL^{-1}$)	%Recovery
TC	1.20	1.22±0.01	101.5±0.5	1.20	1.22±0.04	101.5±3.3
	2.40	2.43±0.02	101.4±0.8	2.40	2.41±0.03	100.4±1.3
	3.60	3.56±0.06	98.7±1.6	3.60	3.53±0.09	97.9±2.4
	4.81	4.82±0.05	100.3±1.1	4.81	5.91±0.06	101.0±1.3
CTC	1.29	1.25±0.01	96.9±0.4	1.29	1.26±0.03	97.4±2.7
	2.58	2.55±0.05	98.8±1.9	2.58	2.53±0.04	98.2±1.5
	3.86	3.80±0.00	98.5±0.0	3.86	3.80±0.09	98.6±2.4
	5.15	5.22±0.03	101.4±0.6	5.15	5.22±0.06	101.4±1.2
OTC	1.24	1.19±0.02	95.6±1.2	1.24	1.17±0.06	94.5±4.8
	2.48	2.41±0.07	97.1±2.7	2.48	2.36±0.08	95.1±3.0
	3.73	3.68±0.06	98.7±1.6	3.73	3.73±0.06	100.2±1.6
	4.97	4.98±0.01	100.2±0.2	4.97	5.05±0.08	100.7±1.6
DC	0.96	0.9±0.0	97.5±2.2	0.96	0.92±0.03	94.1±3.7
	1.92	1.86±0.03	96.4±0.0	1.92	1.92±0.06	100.2±2.9
	2.89	2.78±0.08	96.0±2.7	2.89	2.89±0.10	99.9±3.3
	3.85	3.97±0.06	103.2±1.7	3.85	3.87±0.09	100.6±2.3

4.1.3 Determination of TCs using HPLC with amperometric detection

4.1.3.1 Chromatographic conditions

The first thing to consider in HPLC techniques that must be choosing the separation system. The selection of column type as well as composition of mobile phase system is dependent on the type of analyte ions. In this system, C_{18} column was used as the separation column. Previous works [112-114] used the reversed phase system and added an organic modifier into the aqueous solvent. Three organic modifier have been used, methanol, propanol, and acetonitrile. In this research, the acetonitrile was used as the organic modifier in the mobile phase because the previous literature [113,114] suggested that it gave more symmetrical peaks as well as higher plate efficiencies.

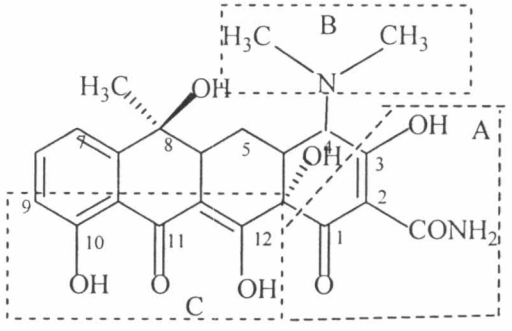

Figure 4.8 TC structure [111].

TCs are derived from a system of four six-membered rings arranged linearly, with a characteristic of double bonds. TCs contain three distinct groups as shown in Fig. 4.8 including the tricarbonyl methane system (A), the dimethyl amino group (B), and the phenolic diketone (C) system. In strongly acidic pH (pH 1-2.5), the TC molecule exists in the fully protonated charge. The fully positively charged TCs at pH 2 provide the highest response as mention in the section 4.1.1.2. However, many reverse-phase packing materials are unstable at pH < 2 resulting in a short column life [112]. Hence, the pH 2.5 was chosen to maintain the column lifetime as well as to avoid the formation of isomeric anologues, which occur rapidly in alkaline medium.

The effect of the buffer system (i.e. potassium dihydrogen phosphate (pH 2.5), Britton-Robinson buffer (pH 2.5), and phosphoric acid (pH 2.5)) as well as the composition of mobile phase were also studied, as shown in Fig. 4.9 – 4.11.

Firstly, potassium dihydrogen phosphate (pH 2.5) containing different ratios of acetonitrile (20-40%) was used as the mobile phase for the chromatography separation of the four TCs. The results found that the higher the ratio of organic modifier, the lower the retention time of all TC compounds, especially CTC, and DC. Hence, 22 % of acetonitrile was the optimum composition for the baseline separation of TCs with a separation time of about 21 min.

The experiments were also carried out using Britton Robinson buffer containing acetonitrile (20-35%). Similar behavior and elution order were obtained. Thirty percent of acetonitrile was the best composition for the baseline separation of TCs with the separation time of about 30 min.

Phosphoric acid (pH 2.5) containing the ratios of acetonitrile 20 % was used as the mobile phase for the chromatography separation of the four TCs using the different flow rate including 0.8, 0.9, and 1 mL min^{-1}. The results found that the flow rate of 0.8 mL min^{-1} was the optimum condition for the baseline separation of TCs with the separation time of about 23 min.

Electrochemical detection needs a mobile phase containing an electrolyte with low ionic strength to provide adequate conductivity and minimize background current [75]. Potassium hydrogen phosphate (pH 2.5) offered the best resolution as well as the highest current response for TC compounds, compared with other electrolytes tested. However, the response peak of doxycycline was not symmetric, and phosphoric acid (pH 2.5) was chosen as an alternative. The final concentration of acetonitrile chosen for the mobile phase was 20% with a flow rate 0.8 mL min^{-1}, which allowed the tetracyclines to elute with favorable retention time and adequate resolution. The separation time was about 23 min.

The elution order of OTC, TC, CTC, and DC can be explained as follows. Due to the same charge and similar structure of the four TCs, the elution sequence was mainly dependent on the hydrophobic interaction that is depicted by by the degree of lipophilicity or P value (the partition coeffiecient in octanol-water at 2.1). The lipophilicity was defined by the molecule having a tendency to dissolve in fat-like (e.g. hydrocarbon) solvent. The elution order of OTC, TC, CTC, and DC

also agreed with their P values which were 0.0035, 0.014, 0.15 and 0.52, respectively [115]. DC was the strongest lipophilic analyte of the above four TCs, and it was the last to elute.

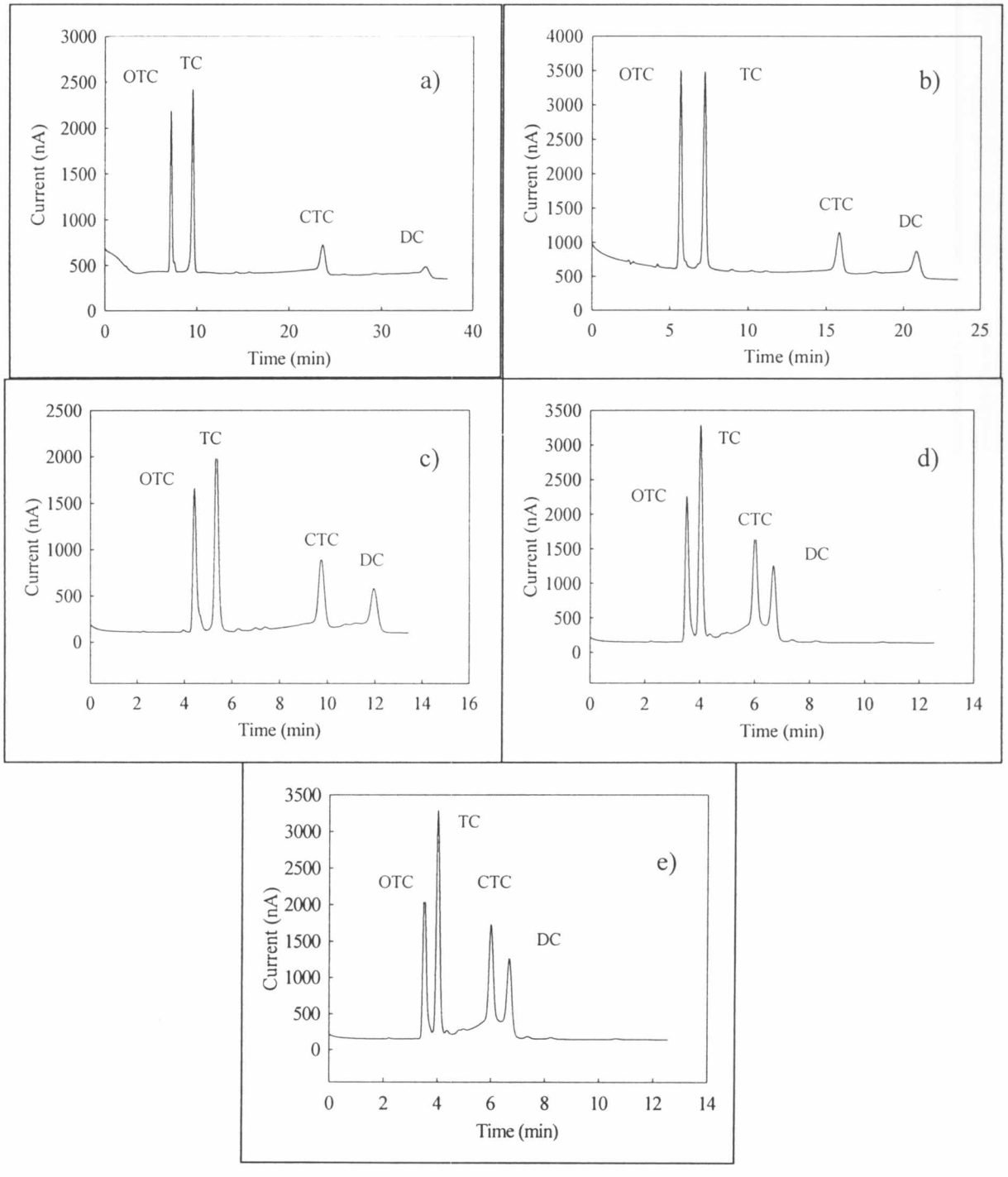

Figure 4.9 Chromatograms of 50 ppm of four TCs in a) 20 : 80 acetonitrile : 0.1 M phosphate buffer (pH 2.5), b) 22 : 78 acetonitrile : 0.1 M phosphate buffer (pH 2.5), c) 25 : 75 acetonitrile : 0.1 M phosphate buffer (pH 2.5), d) 30 : 70 acetonitrile:0.1 M phosphate buffer (pH 2.5), and e) 35 : 65 acetonitrile : 0.1 M phosphate buffer (pH 2.5

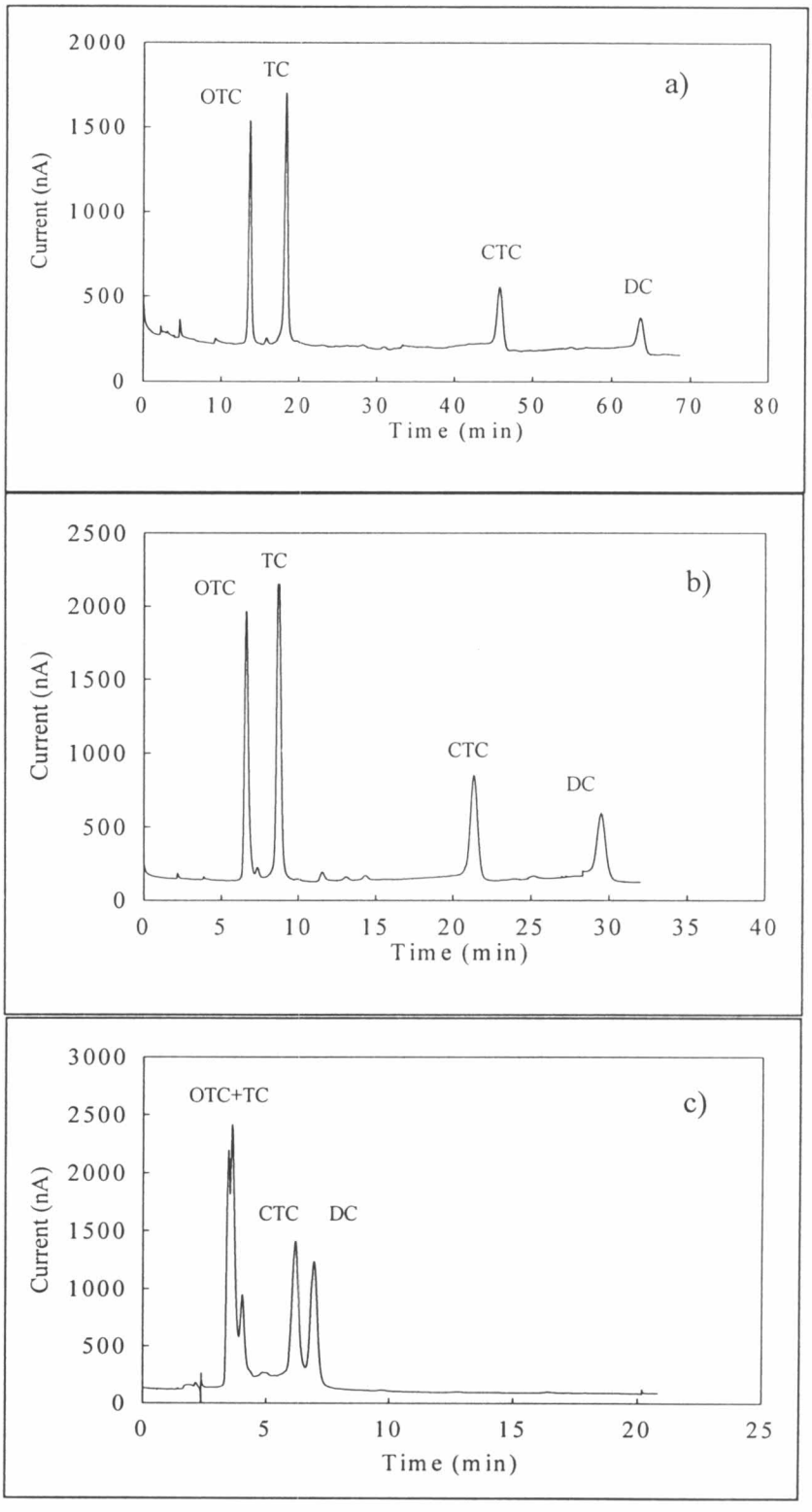

Figure 4.10 Chromatograms of 50 ppm of four TCs in (a) 20 : 80 acetonitrile : 0.04 M Britton Robinson buffer (pH 2.5), b) 30 : 70 acetonitrile : 0.04 M Britton Robinson buffer (pH 2.5), and c) 35 : 65 acetonitrile : 0.04 M Britton Robinson buffer (pH 2.5).

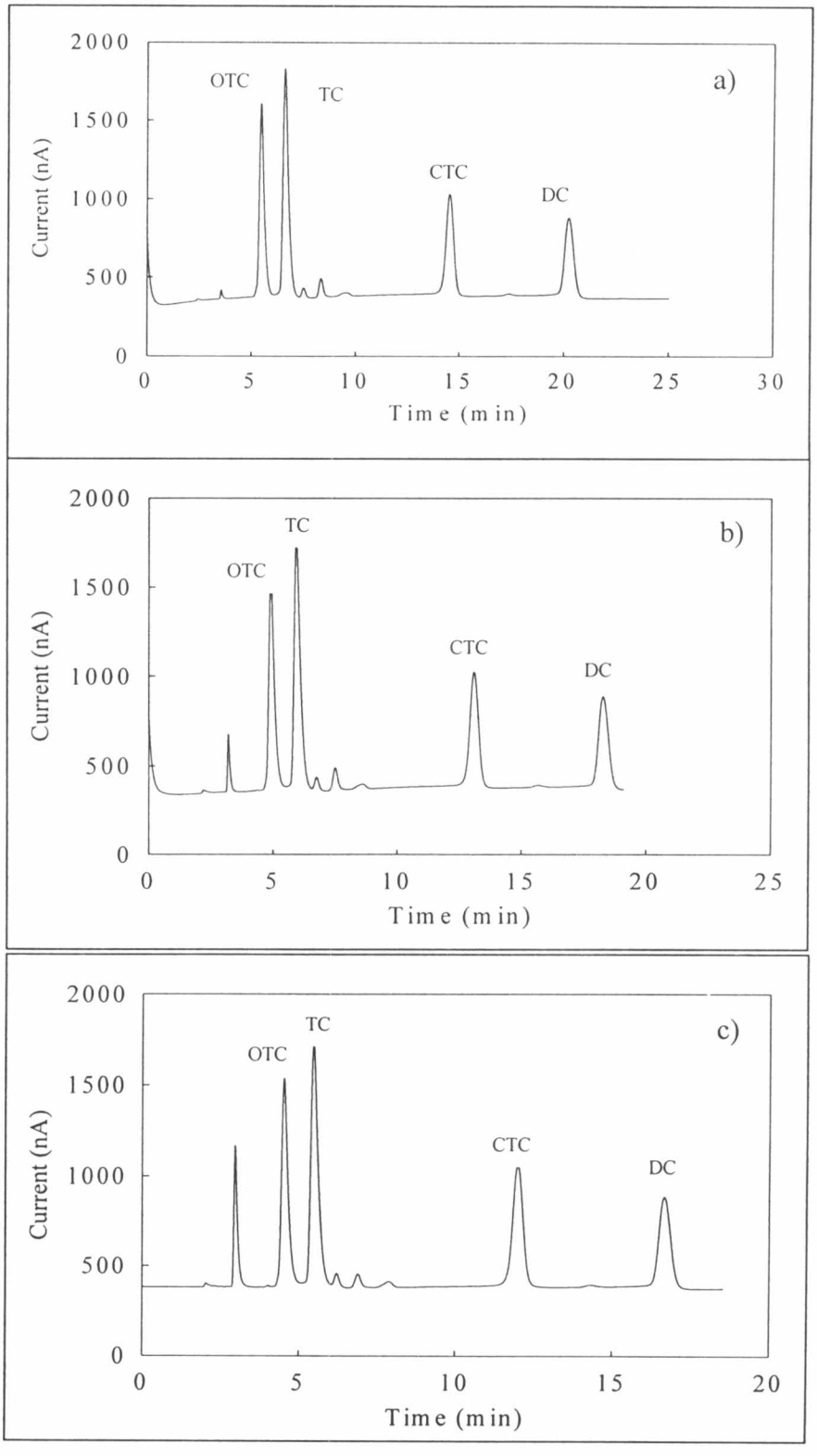

Figure 4.11 Chromatograms of 50 ppm of four TCs in 20:80 acetonitrile : 0.01 M phosphoric acid (pH 2.5) a) 0.8 mL min^{-1} b) 0.9 mL min^{-1}, and c) 1 mL min^{-1}.

4.1.3.2 Hydrodynamic voltammetry of four TCs by HPLC

To obtain the optimum potential, hydrodynamic voltammertry of the four TCs in HPLC was investigated. A hydrodynamic voltammogram was obtained from the average of three injections aliquot of the 20 μL of 100 μM TCs solutions in the HPLC at increasing values of the applied potential from 1.3 to 1.7 V vs. Ag/AgCl. Fig. 4.12 shows the hydrodynamic voltammetric i-E curves obtained from the four TCs. The oxidation current increased in potential until 1.6 V vs. Ag/AgCl for OTC and TC and 1.5 V vs. Ag/AgCl for CTC and DC. Hence, the applied potential at 1.6 V vs. Ag/AgCl was selected for oxidation of the four TCs in the HPLC system.

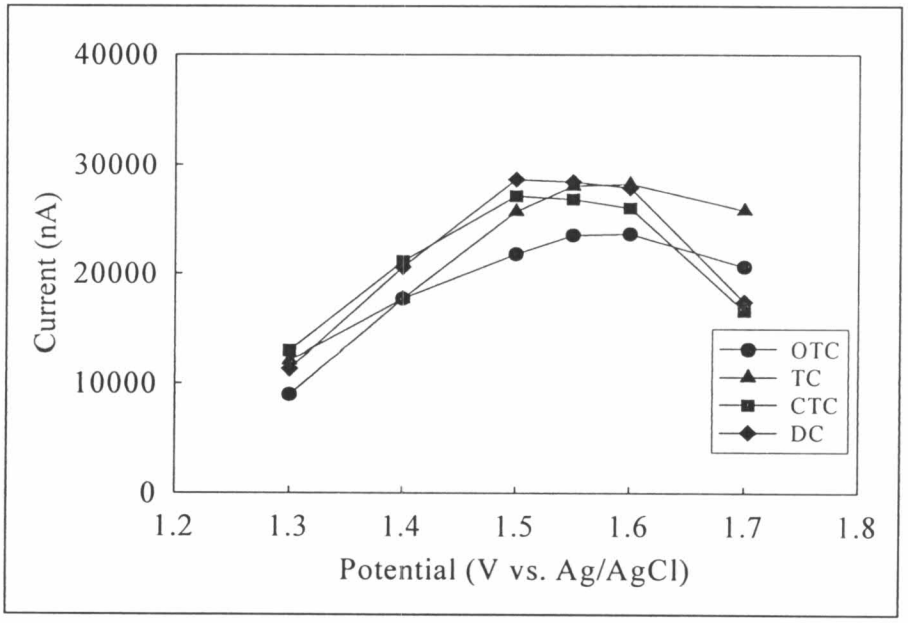

Figure 4.12 Hydrodynamic voltammograms of 50 ppm of four TCs (OTC, TC, CTC, and DC) in 20:80 acetonitrile:0.01 M phosphoric acid (pH 2.5). The flow rate was 0.8 mL min^{-1}.

4.1.3.3 Analytical performance of the HPLC at anodized BDD electrode

Calibration curves of each drug were constructed in the concentration range of 0.01 to 200 ppm (Fig. 4.13). The slope and y-axis intercepted together, with the correlation coefficient were calculated according to a regression equation in the form of (y = mx+b) and summarized as shown in Table 4.7. The calibration graphs of peak-area (in nA) versus concentration (in μg mL^{-1}) showed a linear relationship of 0.05 and 20 ppm for OTC and TC and 0.05 and 100 ppm for CTC and DC.

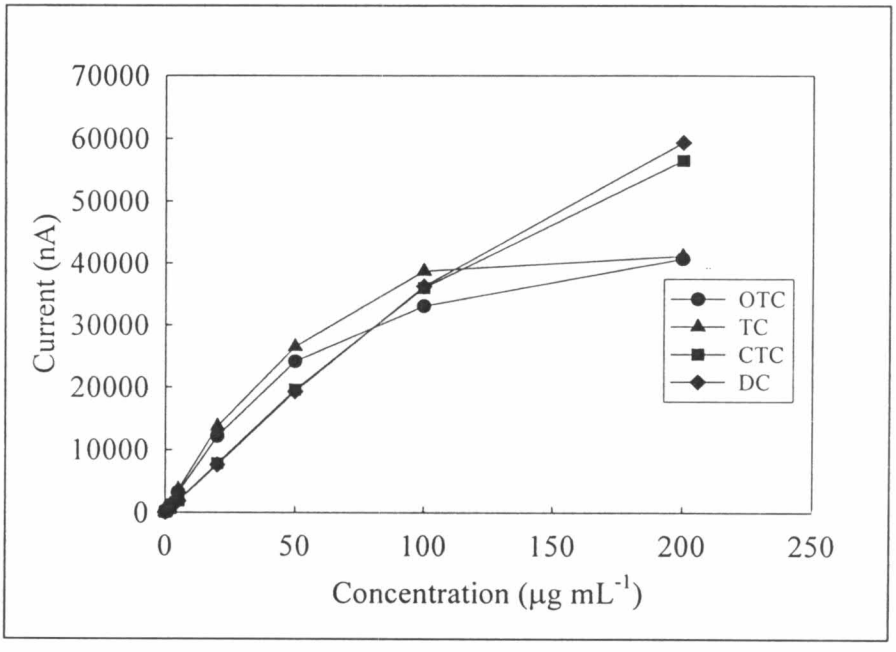

Figure 4.13 Calibration curve of four TCs (OTC, TC, CTC, and DC) in 20:80 acetonitrile : 0.01 M phosphoric acid (pH 2.5). The flow rate was 0.8 mL min^{-1}.

The linear ranges of OTC and TC were narrow, which was probably due to the separation not being adequate for a concentration of higher than 20 ppm. Therefore, the percent of acetonitrile (Fig. 4.14) was decreased, and the final percentage of mobile phase was 19%, which improved in the resolution between OTC and TC when using the high concentration. Retention times of each TC were shown in Table 4.8. From the new condition, the linear dynamic range extended to 50 ppm for OTC and TC, 100 ppm for CTC, and 200 ppm for DC. Table 4.9 summarizes the regression parameters of each drug determination in the new condition.

Table 4.7 Regression analysis of[a] parameters for the determination of TCs in 0.01 M acetonitrile : 0.01 M phosphoric acid (pH 2.5) (20 : 80) using an anodized BDD electrode (n=2) in the HPLC system.

Analytes	Linear range ($\mu g\ mL^{-1}$)	a	b	r^2	LOD (ppm)	LOQ (ppm)
OTC	0.01-20	703.56±14.88	-4.98±9.74	0.9968±0.0006	0.0025	0.0080
TC	0.01-20	76.93±3.87	0.59±11.88	0.9998±0.0001	0.0025	0.0080
CTC	0.01-100	90.23±2.99	9.44±44.03	0.9991±0.0011	0.0050	0.0170
DC	0.01-100	390.02±33.65	63.10±55.66	0.9995±0.0006	0.0050	0.0170

[a] y = ax+b, where y = current (nA), x = concentration (ppm), a = slope (nA ppm^{-1})

Table 4.8 Retention times of four TCs under the following HPLC condition (mobile phase ratio of 19 : 81 acetonitrile : 0.01 M phosphoric acid (pH 2.5)).

Analytes	Retention time (min)
OTC	5.43
TC	6.95
CTC	16.68
DC	23.73

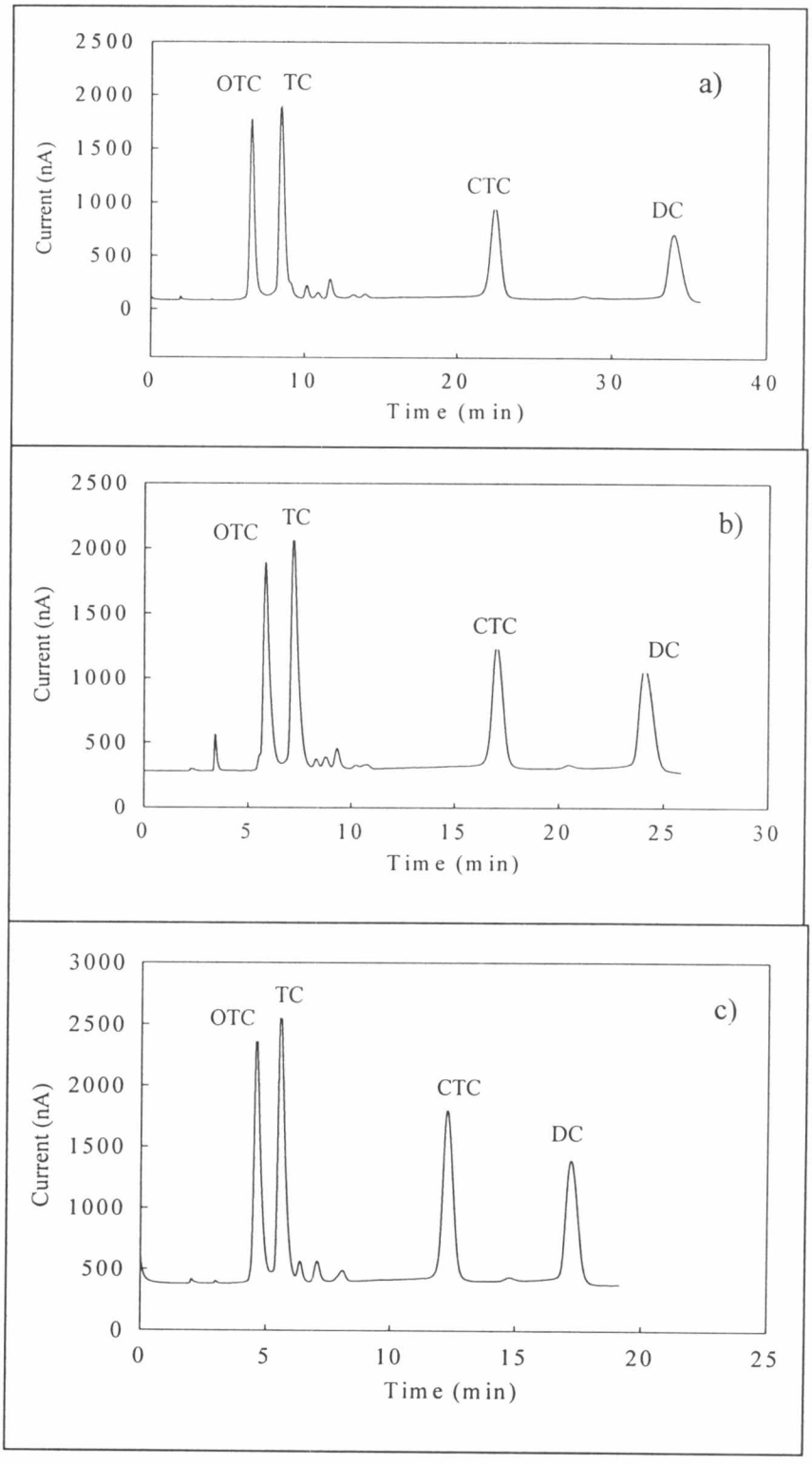

Figure 4.14 Chromatograms of 100 ppm of four TCs in (a) 18 : 82 acetonitrile : 0.01 M phosphoric acid (pH 2.5), b)19 : 81 acetonitrile : 0.01 M phosphoric acid (pH 2.5), and c) 20 : 80 acetonitrile : 0.01 M phosphoric acid (pH 2.5).

Table 4.9 Regression analysis of[a] parameters for the determination of TCs in acetonitrile : 0.01 M phosphoric acid (pH 2.5) (19 : 81) using an anodized BDD electrode (n=2) in the HPLC system.

Analytes	Linear range (ppm)	a	b	r^2	LOD (ppm)	LOQ (ppm)
OTC	0.01-50	518.26±3.58	344.68±51.87	0.9970±0.0002	0.0025	0.0080
TC	0.01-50	600.26±1.97	383.52±19.07	0.9971±0.0004	0.0025	0.0080
CTC	0.01-100	447.43±6.41	49.08.±6.21	0.9981±0.0002	0.0050	0.0170
DC	0.01-200	381.70±13.51	619.77±142.81	0.9966±0.0037	0.0050	0.0170

[a] $y = ax+b$, where y = current (nA), x = concentration (ppm), a = slope (nA ppm^{-1})

The LOD was 0.0025 ppm for OTC and TC and 0.0050 ppm for CTC and DC, and the limit of quantitation (LOQ) was 0.008 ppm for OTC and TC and 0.0017 ppm for CTC and DC. The LOD could not be achieved at the level as low as that obtained from some reports that used LC-MS at the ppb or sub-ppb level. However, the EU has laid down a maximum residue limit (MRLs) for OTC, TC and CTC, which has been set at 100 ng/g in the muscle, 200 ng/g in eggs, 300 ng/g in the liver, and 600 ng/g in the kidney, in order to protect humans from exposure to TCs in edible products of animal origin. Therefore, although the LOD here is not as low as that in the LC-MS system, its values are still adequate for the detection of TCs in food and more cost effective than the LC-MS system.

To check the repeatability of the proposed method, the experiments were carried out by injecting 10 replicates of the four TCs at the concentration of 10 ppm. The peak variability defined as the relative standard deviation (%RSD), was 3.0, 3.1, 2.6, and 3.2 % for OTC, TC, CTC, and DC, respectively.

4.1.3.4 Application of the determination TCs in egg samples

The proposed calibration curve method was applied for the determination of each TCs in eggs. Egg samples were purchased from a local market. and the various extraction methods are explained in experiment section 3.7.4. The results of percentage recovery of each extraction are shown in Table 4.10.

Initially, the AOAC extraction and cleanup method was used to determine the TCs in animal tissues using Mcvaille-EDTA buffer (pH 4) as the extraction reagent and SPE for cleanup of the sample. However, this method failed because the egg samples were not deprotenized in the Mcvaille-EDTA buffer that induced the formation of colloidal in the extraction buffer. Therefore, the colloidal in the extraction buffer could not pass through the SPE cartridge.

The requirement of the deproteinized step was necessary for the separation and extraction of TCs from the egg samples. Three extraction reagents including perchloric acid (aqueous solution), acetonitrile (moderated polar organic solvent) and ethyl acetate (non-polar organic solvent) were used. Recovery data were summarized in Table 4.10. Discharging the organic waste is a severe problem, extraction method should be avoided. A small amount of perchloric acid as the extraction reagent is an alternative choice for the extraction. However, this method produced poor recoveries and reproducibility (Fig. 4.15). Thus, acetonitrile was chosen as the alternative choice for this purpose. The key to this extraction is the mixing step between the solvent and sample. Three mixing procedures including a hand shaker, mechanical shaker and magnetic stirrer were used (Fig.4.16 - 4.18). The magnetic stirrer provided the best recovery because it could increase the surface area of and improve the solvent penetration through the sample, thus resulting in the improvement of solvent extraction. Ethyl acetate was also used as an extraction reagent for comparison (Fig. 4.19). From these results, the extraction using acetonitrile provided the best recovery for the four TC. Hence, acetonitrile was used for extraction of the TCs in egg samples.

Recoveries of TCs in egg samples were studied by spiking mix standard solution of 0.5, 1, 5, and 10 ppm in the egg samples. The precision and reproducibility were based on intra-assay and inter-assay. The data are summarized in Table 4.11 and 4.12. Recovery of the four TCs obtained for the intra-assay study was 84.67-104.4 %, 75.3-84.9%, 83-102.5 %, and 88.6-103.2 % for OTC, TC, CTC

and DC, respectively. The inter-assay study was also established by spiking four mixing standard solutions in 3 days. Recovery of the four TCs obtained for inter-assay study were 84.7-110.6 %, 70.1-88.6 %, 86.7-102.5 %, and 86.8-103.2 % for OTC, TC, CTC, and DC, respectively. The standard deviations of recoveries obtained were high especially in the low concentration of spiked standard solution. This was probably due to the difference in water contents in the residue of each sample. The TCs in the water provided a higher response signal than those in the organic solvent, and induced an error of the percent recoveries.

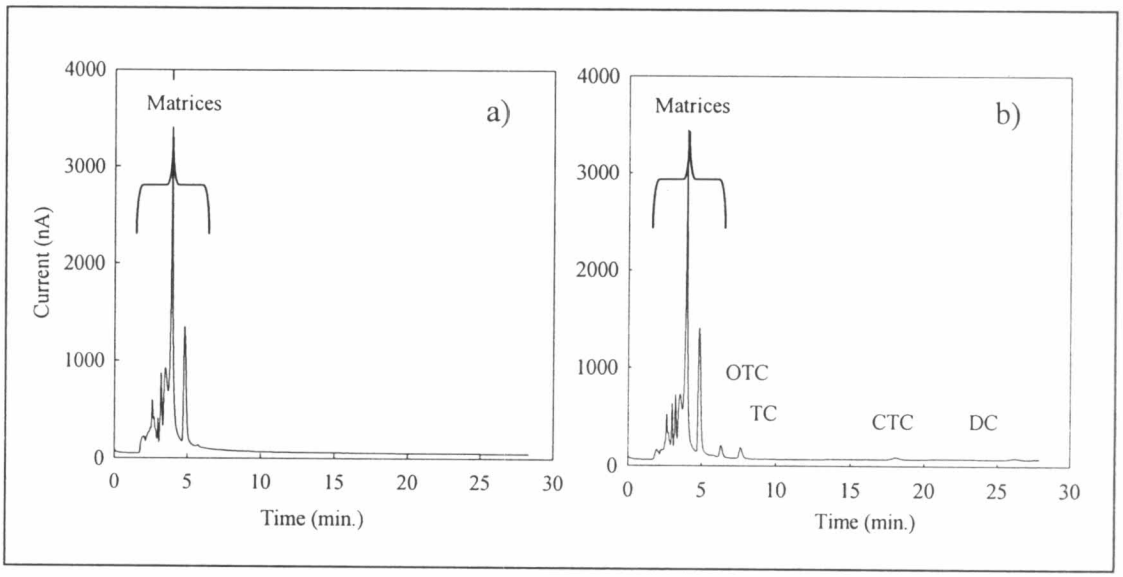

Figure 4.15 Chromatograms of egg samples a) blank egg and b) spiked 5 ppm standard using perchloric acid (method II) as the extraction reagent.

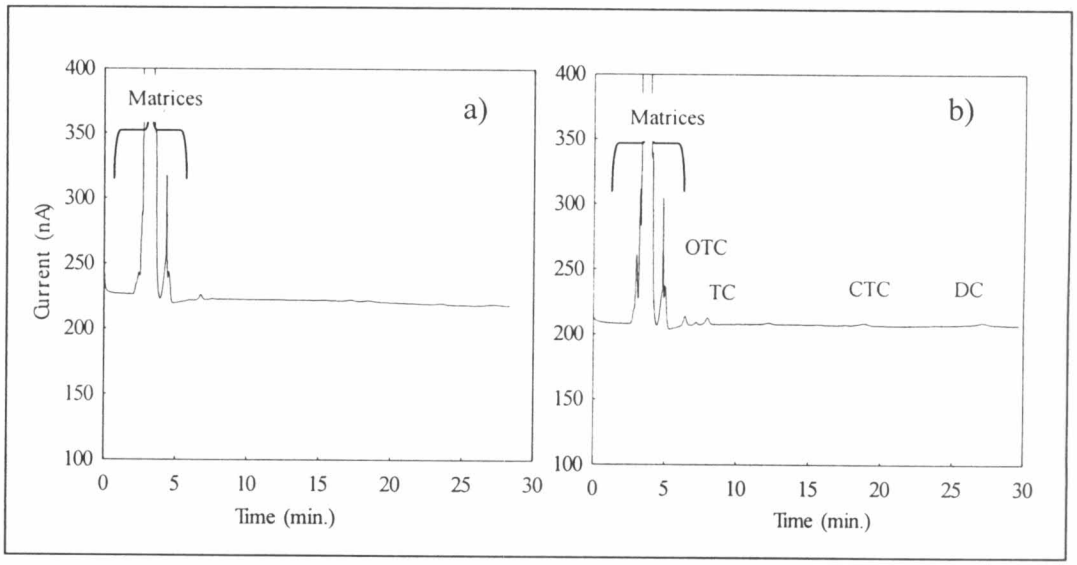

Figure 4.16 Chromatograms of egg samples a) blank egg and b) spiked 5 ppm standard using acetonitrile (method III) as the extraction reagent (hand shaker).

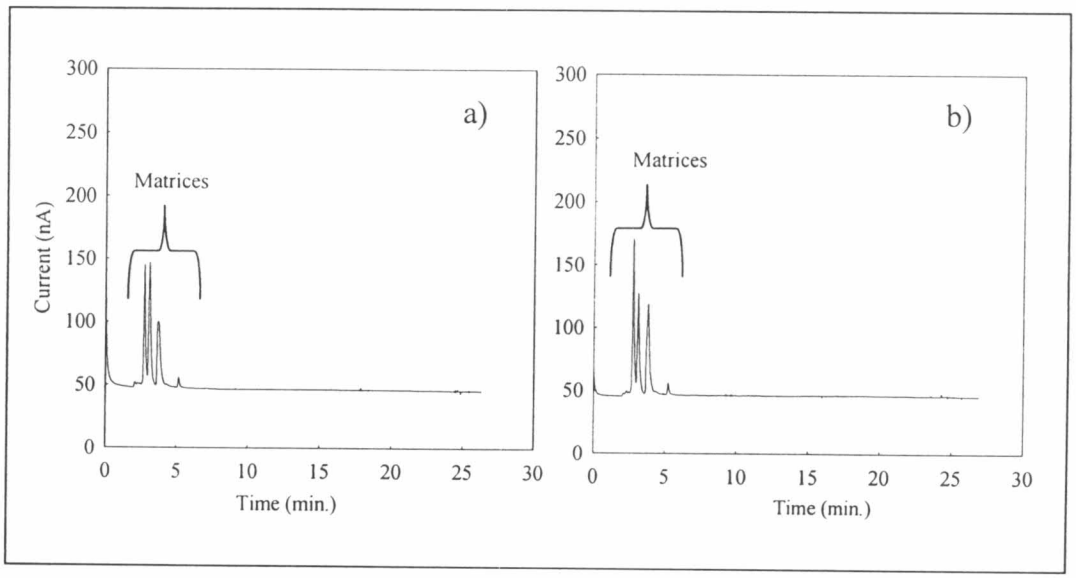

Figure 4.17 Chromatograms of egg samples a) blank egg and b) spiked 5 ppm standard using acetonitrile (method III) as the extraction reagent (mechanical stirrer).

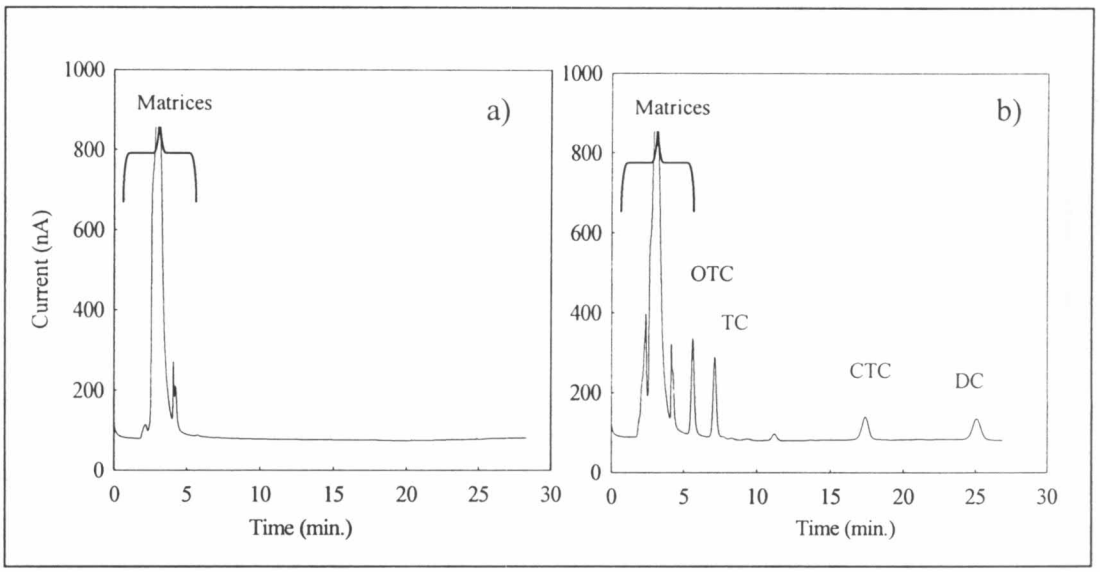

Figure 4.18 Chromatograms of egg samples a) blank egg and b) spiked 5 ppm using acetonitrile (method III) as the extraction reagent (magnetic stirrer).

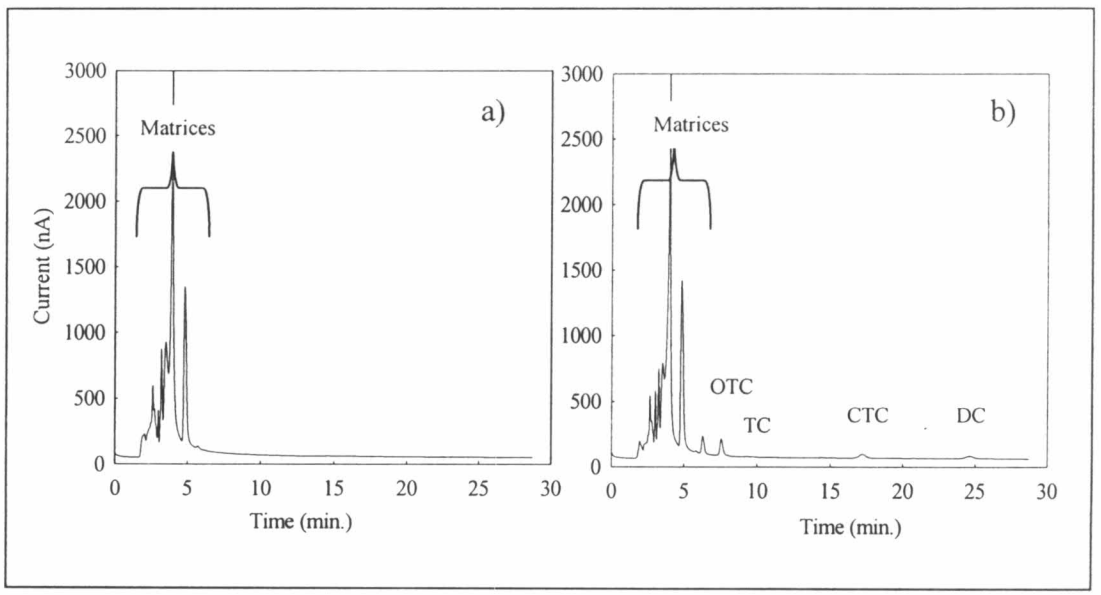

Figure 4.19 Chromatograms of egg samples a) blank egg and b) spiked 5 ppm using ethyl acetate (method IV) as the extraction reagent.

Table 4.10 Recovery data of spiked standard in blank eggs using various sample preparation methods.

Methods	Concentrations	Percentage recovery (average±sd) (n = 2)			
		OTC	TC	CTC	DC
Perchloric acid	5 μg mL^{-1}	42.3±2.4	32.7±0.2	40.0±5.0	34.6±6.2
	10 μg ml^{-1}	26.5±3.9	26.7±5.9	27.4±8.0	23.1±8.6
Acetonitrile (hand shaker)	5 μg mL^{-1}	6.3±0.3	4.8±1.5	5.7±0.1	10.8±2.8
	10 μg mL^{-1}	5.2±0.1	7.2.±0.1	3.2±0.1	4.3±0.2
Acetonitrile (mechanical shaker)	5 μg mL^{-1}	ND*	ND*	ND*	ND*
	10 μg mL^{-1}	ND*	ND*	ND*	ND*
Acetonitrile (magnetic stirrer)	5 μg mL^{-1}	103.4±1.4	86.7±2.6	100.6±1.5	101.8±0.9
	10 μg mL^{-1}	98.5±3.1	85.3±0.5	94.0±4.1	99.8±3.7
Ethyl acetate	5 μg mL^{-1}	89.0±1.7	72.8±1.2	105.6±0.9	104.4±0.1
	10 μg mL^{-1}	84.33±1.2	72.3±1.4	110.86±4.9	104.4±2.2

*ND-not detectable

Table 4.11 Recovery data of spiked standard (intra-day assay) in blank eggs using acetonitrile as the extraction reagent.

Concentrations (μg mL^{-1})	Percentage recovery (average±sd) (n = 2)			
	OTC	TC	CTC	DC
0.5	95.1±2.1	76.9±2.3	89.7±1.6	93.2±0.5
1	88.6±3.1	73.8±2.4	83.8±1.2	89.5±1.3
5	103.4±1.4	86.7±2.6	100.6±1.5	101.8±0.9
10	101.6±1.2	85.2±0.4	94.0±4.1	97.8±3.7

Table 4.12 Recovery data of spiked standard (inter-day assay) in blank eggs using the acetonitrile as the extraction reagent.

Concentrations ($\mu g\ mL^{-1}$)	Percentage recovery (average±sd) (n = 6)			
	OTC	TC	CTC	DC
0.5	97.9±4.9	77.5±6.1	88.4±1.4	93.5±1.2
1	88.6±3.1	80.4±5.3	84.4±1.2	88.9±1.3
5	106.4±3.7	86.7±2.3	100.6±1.4	103.2±1.9
10	104.0±4.9	84.0±1.4	95.9±3.2	97.8±3.7

4.2 Determination of hydrogen peroxide using chromium (III) hexacyanoferrate (II) modified BDD electrode

Prussian Blue, or ferric hexacyanoferrate is one of the most ancient coordianation material found in the beginning of the eighteen century. However, the use of Prussian Blue film onto the electrode surface as electroactive layers is blocked in the presence of some cation i.e. Na^+, H^+, and Li^+ and sensitive to the pH. A few years later, other metal hexacyanoferrate have been found to deposite on various electrode surfaces. Recently, the electro-deposition of chromium hexacyanoferrate has been reported [106]. The present study focused on the development of sensor for the hydrogen peroxide determination based on chromium (III) hexacyanoferrate (II) modified BDD electrode. The study was separated into 3 parts including the finding of the optimum condition for the preparation of chromium hexacyanoferrate on BDD electrode, cyclic voltammetry and flow injection with amperometric detection. The details of each part were described as the follows.

4.2.1 Preparation of chromium (III) hexacyanoferrate (II) on BDD electrode

In this topic, the effect of many parameters including electrode pretreatment methods, electro-deposition methods, and mole ratio between the chromium nitrate, and potassium hexacyanoferrate were investigated in order to find the optimum condition that provide the excellent sensitivity of sensor.

4.2.1.1 Effect of electrode pretreatment methods.

In this study, several electrode pretreatment methods wer carried out in order to improve the electrode surface for the binding of chromium (III) hexacyanoferrate (II) on the electrode surface. The details of each method were described as the following:

4.2.1.1.1 As-deposited BDD electrode In this experiment, no electrode pretreatment was used.

4.2.1.1.2 Anodized BDD electrode treated with potassium

hydroxide. The electrode was pretreated with 0.1 M potassium hydroxide solution and cycling from 0 to 2.4 V vs. Ag/AgCl for 1 hour at the scan rate 0.01 V/s.

4.2.1.1.3 Anodized BDD electrode treated with sulfuric acid. The electrodes were pretreated with 0.1 M sulfuric acid and cycling from -2 to 2 V vs. Ag/AgCl for 0.5, 1, and 1.5 hrs. at the scan rate 10 mV s^{-1}.

4.2.1.14 Anodized BDD electrode treated with sulfuric acid (fixed current 20 min). The electrode was pretreated with 0.1 M sulfuric acid using potentiometry with fixed current 10 mV cm^{-2} for 20 min.

4.2.1.1.4 Anodized BDD electrode treated with sulfuric acid (abrasive electrode). The electrodes were pretreated with 0.1 M sulfuric acid and cycling from -2 to 2 V vs. Ag/AgCl for 1 hr. at the scan rate 0.01 V/s. Before the anodization of electrode with sulfuric acid, the electrode was abrasive 1 time with the abrasive paper no Cw-1000.

4.2.1.1.5 Anodized BDD electrode treated with potassium hydroxide and sulfuric acid. The electrode was pretreated with 0.1 M potassium hydroxide solution and cycling from 0 to 2.4 V vs. Ag/AgCl for 1 hr. After that, the electrode was pretreated with 0.1 M sulfuric acid and cycling from -2 to 2 V vs. Ag/AgCl for 1 hr.

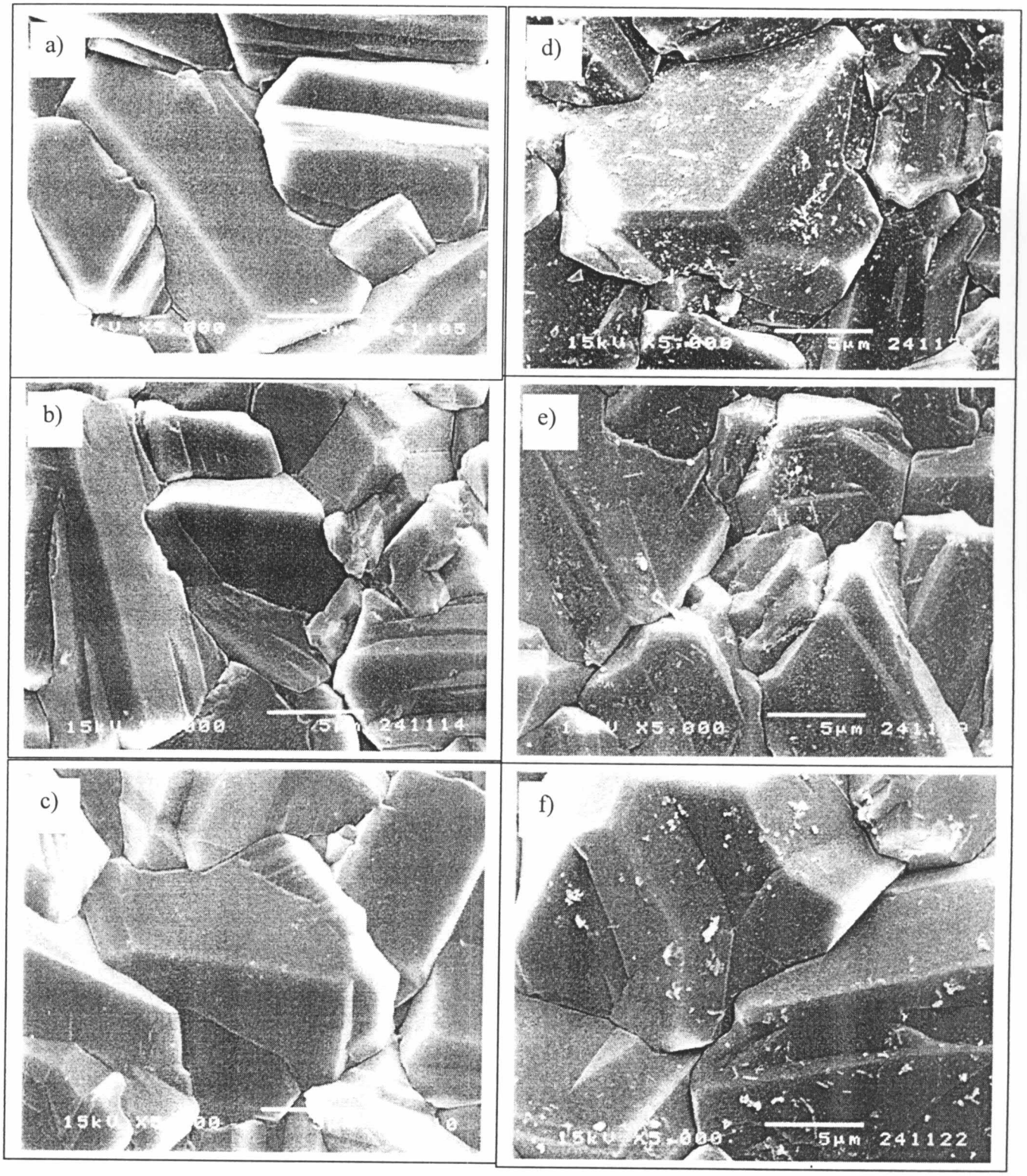

Figure 4.20 SEM a) as-deposited BDD electrode b) anodized BDD electrode treated with 0.1 M sulfuric acid, c) anodized BDD electrode treated with 0.1 M potassium hydroxide, d) chromium (III) hexacyanoferrate (II) modified as-deposited BDD electrode, e) chromium (III) hexacyanoferrate (II) modified anodized BDD electrode treated with 0.1 M sulfuric acid, and f) chromium (III) hexacyanoferrate (II) modified anodized BDD electrode treated with 0.1 M potassium hydroxide.

Fig. 4.20 shows SEM image of BDD, anodized BDD treated with potassium sulfuric acid and anodized BDD treated with potassium hydroxide as well as the chromium (III) hexacyanoferrate (II) modified on each electrode. The BDD film composed of sharp and well-faceted microcrystalline with numerous grain boundaries. After the anodic pretreatment, the surface morphology changed only slightly, exhibiting a low degree of etching that is just barely visible at high magnification with scanning electron microscopy. The change of the surface morphology increased the roughness or porosity on the surface as well as the increasing of the electrode surface resulting in the increasing the catalytic properties [116]. The SEM of chromium (III) hexacyanoferrate (II) modified on each electrode did not give any significant difference.

Table 4.13_ i-E of voltammetric results of 1 mM hydrogen peroxide in 0.1 M potassium chloride (pH 5) using chromium (III) hexacyanoferrate (II) modified BDD electrode treated with different electrode pretreatment methods.

Pretreatment methods	Potential (V vs. Ag/AgCl)	Current (μA)
As-deposited BDD	0.854	1.272
Anodized BDD treated with sulfuric acid (0.5 hr)	0.822	0.400
Anodized BDD treated with sulfuric acid (1.0 hr)	0.858	1.642
Anodized BDD treated with sulfuric acid (1.5 hr)	0.843	1.024
Anodized BDD treated with sulfuric acid (fixed current 20 min)	0.831	1.147
Anodized BDD treated with abrasive and sulfuric acid (1 hr)	0.861	1.266
Anodized BDD treated with potassium hydroxide (1 hr)	0.821	0.923
Anodized BDD treated with sulfuric acid (1 hr) + potassium hydroxide (1 hr)	0.846	1.156

Table 4.13 summarizes the electrochemical parameters of 1 mM hydrogen peroxide using various electrode pretreatment methods. The previous study suggested that the anodic pretreatment of BDD surface in 0.1 M sulfuric acid converse the H-terminated of BDD surface to the O-terminated (carbonyl group) resulting in the negative charge on the anodized BDD surface. The interaction between the transition metal redox coupled on the anodized BDD surface was ion-dipole interaction. These can be either repulsive, in the case of anions, or attractive, in the case of cations. Therefore, the chromium (III) hexacyanoferrate (II), one of the cations mix-valent, is attracted to the negative charge on the anodized BDD surface resulting in the best binding of the chromium (III) hexacyanoferrate (II) on the anodized BDD surface treated with 0.1 M sulfuric acid. From the results, the highest current response was obtained using anodized BDD electrode treated with 0.1 M sulfuric acid for 1 hr. Thus, this pretreatment was used in the rest of the experiments.

4.2.1.2 Effect of electrodeposition methods

The binding characteristics of chromium (III) hexacyanoferrate (II) on the BDD surface was a topic that have been interested in. The electrodepostion is the important step that affects the binding of chromium (III) hexacyanoferrate (II). Thus, several electrodeposition methods were employed to obtain the good binding as the following

4.2.1.2.1 Amperometry: Fix potential at -1 V vs. Ag/AgCl for 1 hr.

4.2.1.2.2 Cyclic voltammetry: Scan potential from -0.2 V to 0.95 V vs. Ag/AgCl for 1 hr

4.2.1.2.3 Pulse amperometry: Potential pulse with the pulse length 0.5 s with the minimum potential -0.2 V vs. Ag/AgCl and maximum potential 0.95 V vs. Ag/AgCl for 1 hr.

Table 4.14 i-E of voltammetric results of 1 mM hydrogen peroxide in 0.1 M potassium chloride (pH 5) using chromium (III) hexacyanoferrate (II) modified BDD electrode using different electrodeposition methods.

Deposition methods	Potential (V vs. Ag/AgCl)	Current (μA)
Amperometry (Fix potential)	0.854	0.883
Cyclic voltammetry	0.858	1.642
Pulse amperometry (Potential pulse)	0.846	0.494

Table 4.14 were summarized the electrochemical parameters of 1 mM hydrogen peroxide in 0.1 M potassium chloride (pH 5) using chromium (III) hexacyanoferrate (II) modified BDD electrode of each electrodeposition method. The use of the potential pulse technique give the poor adherence of cluster layer of chromium hexacyanoferrate , although this method has been successfully employed for the iridium oxide on to the diamond electrode. Our results showed that, among the electrodeposition method investigated, the cyclic voltammetry provided the highest current signal because a less noisy and smooth cluster layer on the BDD electrode surface was obtained. Hence, subsequently all the electrode preparation were carried out by cyclic voltammetry.

4.2.1.3 Effect of molar ratios between chromium nitrate and potassium hexacyanoferrate

Effect of molar ratios between chromium nitrate and potassium hexacyanoferrate on the current response of chromium (III) hexacyanoferrate (II) modified electrodes was investigated (Table 4.15). The catalytic properties of chromium (III) hexacyanoferrate(II) obtained by replacing the Fe(III) with Cr(III) ions during the formation of a mixed-valence compound. The stochiometric of Cr:Fe is 1:1. However, the excess amount of chromium should be added to avoid the formation of Prussian during the formation of chromium (III) hexacyanoferrate(II). From the results, we found that the ratio of 4:1 provided the highest current response. Thus, the ratio of 4:1 was used for the rest of the experiments.

Table 4.15 i-E of voltammetric results of 1 mM hydrogen peroxide using chromium (III) hexacyanoferrate(II)modified BDD electrode using different molar ratios of chromium nitrate and potassium hexacyanoferrate.

Cr:Fe molar ratios	Potential (V vs. Ag/AgCl)	Current (μA)
1:1	0.821	0.747
2:1	0.913	0.897
4:1	0.826	1.379

4.2.2 Cyclic voltammetry of hydrogen peroxide determination

4.2 2.1 pH dependence

The BDD electrode modified with chromium (III) hexacyanoferrate(II) was studied over the pH range between 2 and 9 in a solution containing 1 mM of hydrogen peroxide. Fig. 4.21 shows the effect of pH on the anodic peak current of the modified electrode. It was observed that the anodic peak current increased with the increase of pH until the pH 5, then the current gradually decreased. This behavior was probably because the noise level gradually increases at pH > 7, which attributed to the conversion of chromium (III) hexacyanoferrate (II) to a chromium gel in the pH > 7 [106]. Hence, the pH 5 was used in the rest of the experiment.

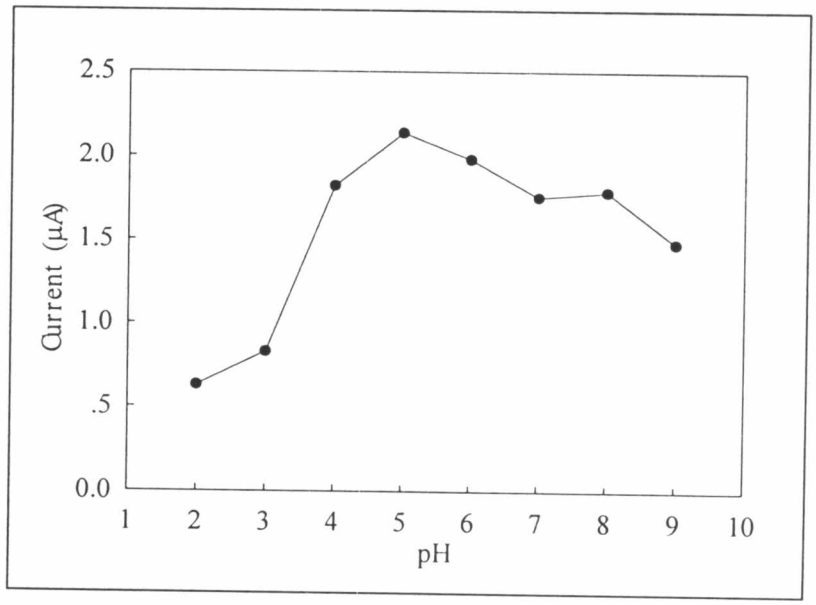

Figure 4.21 Influence of pH on the voltammetric response of the chromium (III) hexacyanoferrate (II) modified BDD electrode in potassium chloride solution containing 1 mM hydrogen peroxide. The scan rate was 50 mV s^{-1}.

4.2.2.2 Effect of electrolyte/buffer systems

Other parameters that effect the response of the chromium (III) hexacyanoferrate (II) modified BDD electrodes for the determination of hydrogen peroxide is electrolyte/buffer system. In this study, several electrolyte systems were used as following:

4.2.2.2.1 Potassium chloride (pH 5) (Fig. 4.22)

4.2.2.2.2 Potassium chloride + Succinic acid (pH 5) (Fig. 4.23)

4.2.2.2.3 Succinic acid (pH 5) (Fig. 4.24)

4.2.2.2.4 Succinic acid + Ammonium chloride (pH 5) (Fig. 4.25)

4.2.2.2.5 Succinic acid + Sodium acetate (pH 5) (Fig. 4.26)

4.2.2.2.6 Acetate buffer (pH 5) (Fig 4.27)

4.2.2.2.7 Phosphate buffer (pH 5) (Fig. 4.28)

4.2.2.2.8 Britton-Robinson buffer (pH 5) (Fig 4.29)

Table 4.16 i-E of voltammetric results of 1 mM hydrogen peroxide in different electrolyte/buffer systems using chromium (III) hexacyanoferrate (II) modified BDD electrodes.

Electrolyte , Buffer	Potential (V vs. Ag/AgCl)	Current (μA)
Potassium Chloride (pH 5)	0.874	1.978
Potassium Chloride + Succinic acid (pH 5)	0.864	1.627
Succinic acid (pH 5)	0.849	1.127
Succinic acid + Ammonium chloride (pH 5)	0.748	1.156
Succinic acid + Sodium acetate (pH 5)	0.864	0.546
Acetate buffer (pH 5)	0.864	0.849
Phosphate buffer (pH 5)	0.892	0.891
Britton-Robinson buffer (pH 5)	0.864	0.651

Table 4.16 summarizes the electrochemical parameters of 1 mM hydrogen peroxide in electrolyte/buffer systems as mention above using chromium (III) hexacyanoferrate (II) modified BDD electrodes. The voltammeteric behavior of hydrogen peroxide using chromium (III) hexacyanoferrate (II) modified BDD electrodes in the solution or the buffer solution containing the alkali-metal ion (potassium ion) exhibited the well-defined cyclic voltammograms. On the other hand, the ill-defined voltammograms were obtained in the solution containing only the buffer system. This behavior can be explained by the previous study [106] that the size of cation and anion have profound effects. Chloride ion provides a greater significant current response than other potassium salts such as potassium nitrate, acetate and phosphate. The potassium was found to be the most suitable cation to use in the electrolyte solution. The potassium ion has the most compatible size for the chloride. The electrolyte studies indicated that potassium chloride provides the best response to the hydrogen peroxide determination. Hence, potassium chloride was used as the electrolyte for the rest of the experiments.

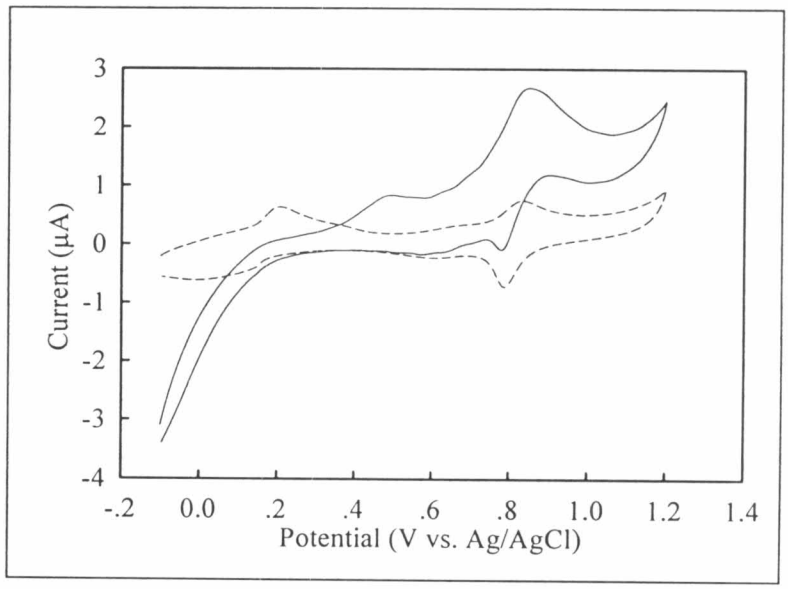

Figure 4.22 Cyclic voltammogram of 1 mM hydrogen peroxide (solid line) in 0.1 M potassium chloride (pH 5) together with the corresponding background current (dashed line) using chromium (III) hexacyanoferrate (II) modified BDD electrode.

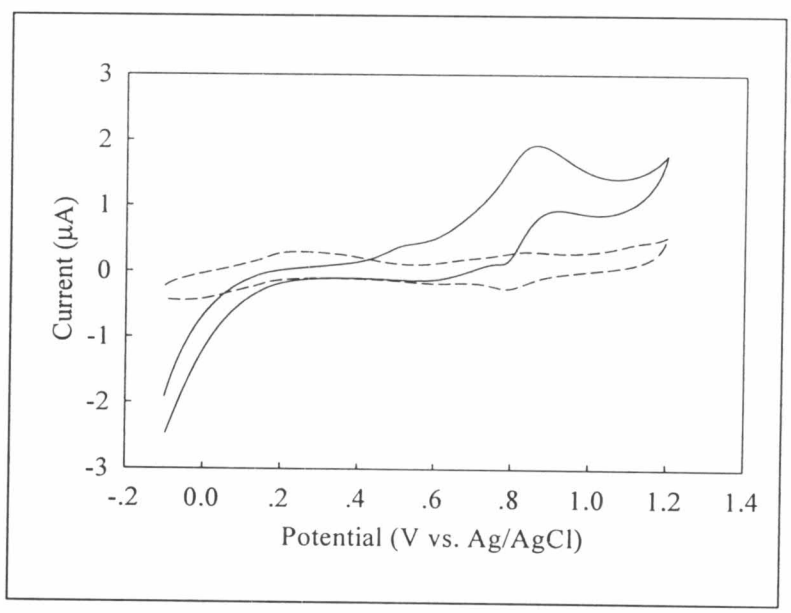

Figure. 4.23 Cyclic voltammogram of 1 mM hydrogen peroxide (solid line) in 0.1 M potassium chloride + 0.1 M succinic acid (pH 5) together with the corresponding background current (dashed line) using chromium (III) hexacyanoferrate (II) modified BDD electrode.

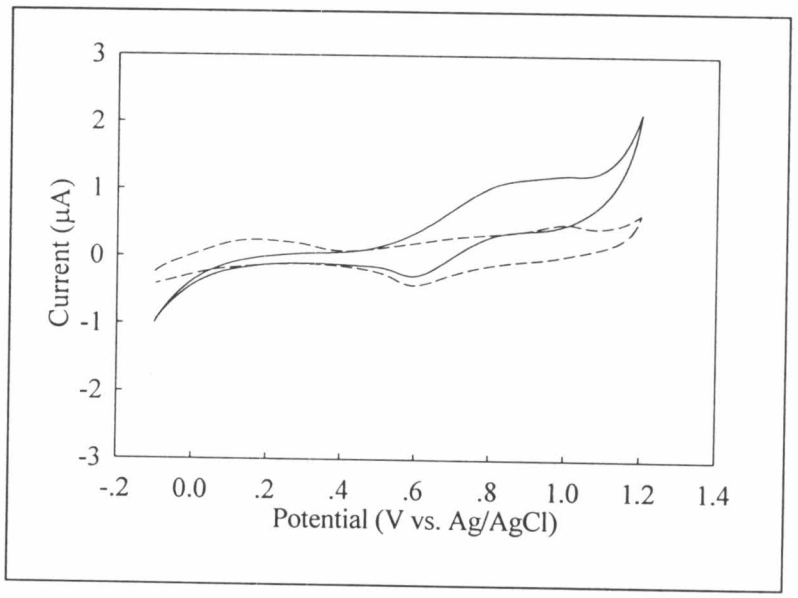

Figure 4.24 Cyclic voltammogram of 1 mM hydrogen peroxide (solid line) in 0.1 M succinic acid (pH 5) together with the corresponding background current (dashed line) using chromium (III) hexacyanoferrate (II) modified BDD electrode.

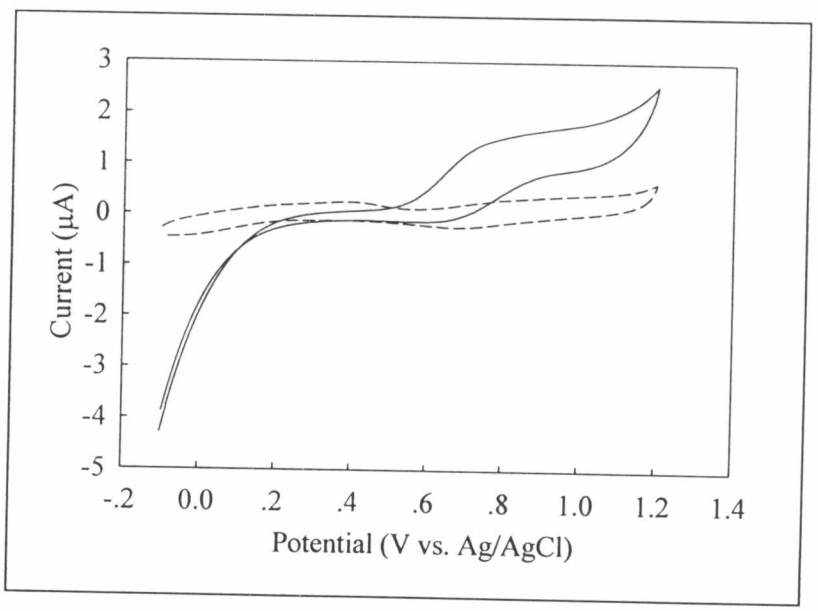

Figure 4.25 Cyclic voltammogram of 1 mM hydrogen peroxide (solid line) in 0.1 M succinic acid + 0.1 M ammonium chloride (pH 5) together with the corresponding background current (dashed line) using chromium (III) hexacyanoferrate (II) modified BDD electrode.

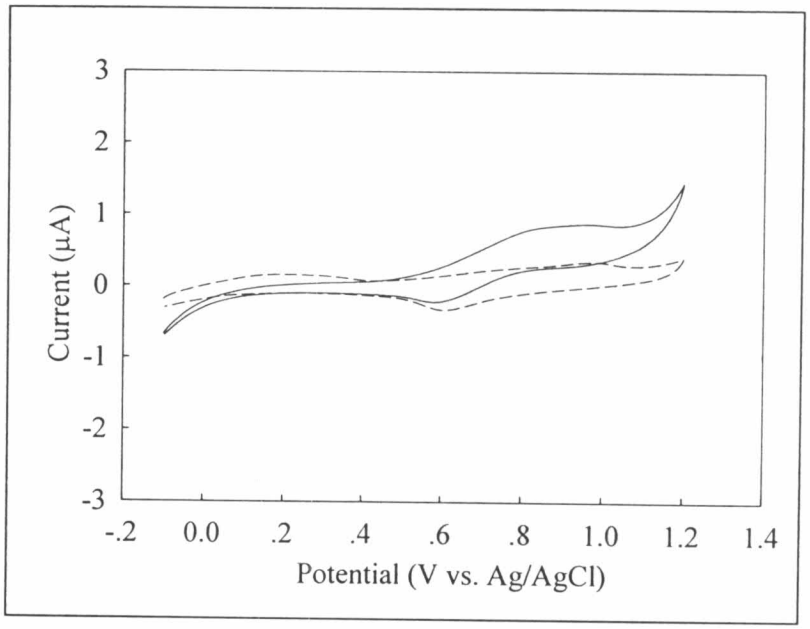

Figure 4.26 Cyclic voltammogram of 1 mM hydrogen peroxide (solid line) in 0.1 M succinic acid + 0.1 M sodium acetate buffer (pH 5) together with the corresponding background current (dashed line) using chromium (III) hexacyanoferrate (II) modified BDD electrode.

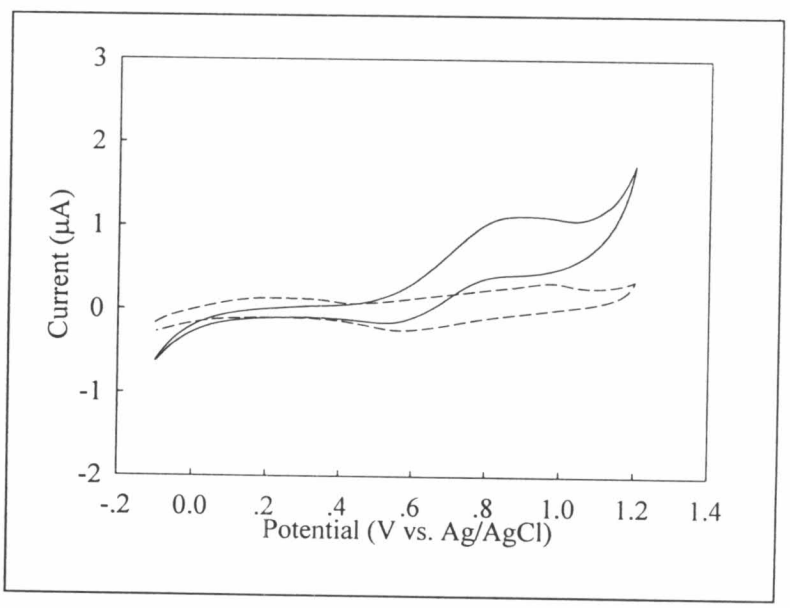

Figure 4.27 Cyclic voltammogram of 1 mM hydrogen peroxide (solid line) in 0.1 M acetate buffer (pH 5) together with the corresponding background current (dashed line) using chromium (III)hexacyanoferrate (II) modified BDD electrode.

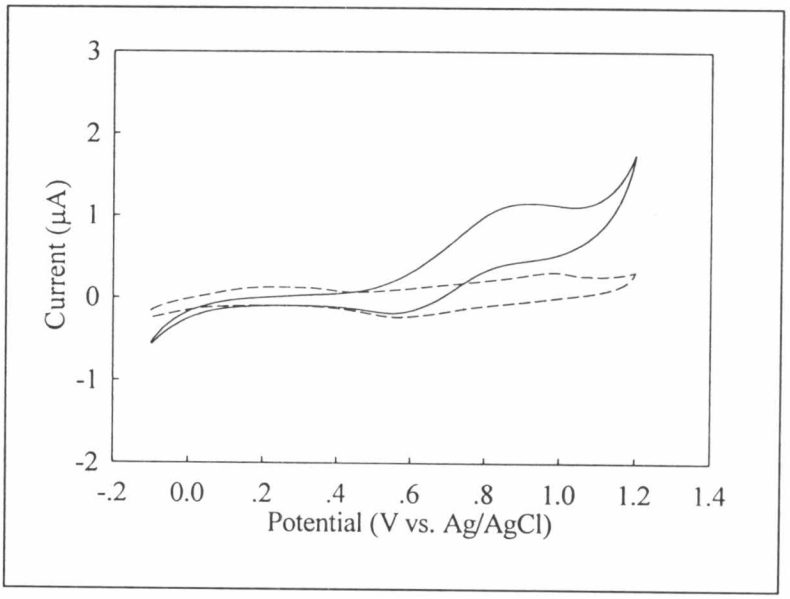

Figure 4.28 Cyclic voltammogram of 1 mM hydrogen peroxide (solid line) in 0.1 M phosphate buffer (pH 5) together with the corresponding background current (dashed line) using chromium (III) hexacyanoferrate (II) modified BDD electrode.

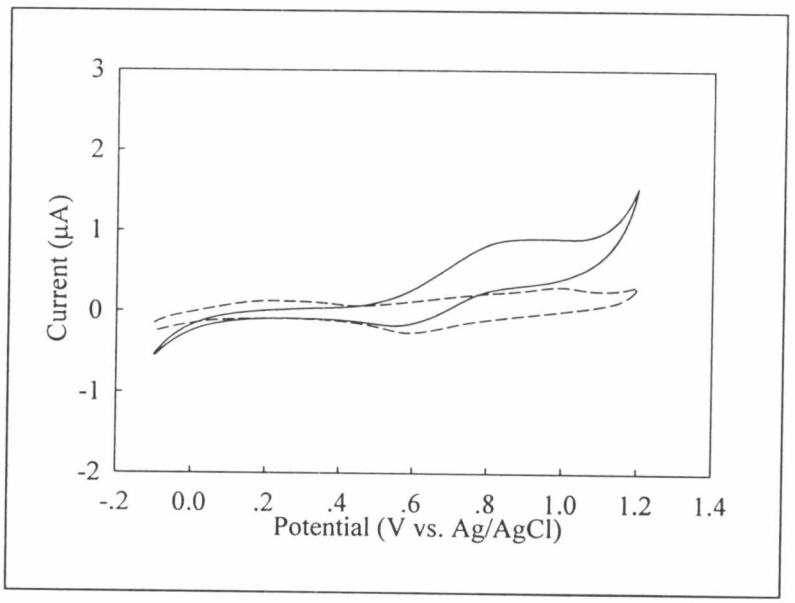

Figure 4.29 Cyclic voltammogram of 1 mM hydrogen peroxide (solid line) in 0.1 M Britton-Robinson buffer (pH 5) together with the corresponding background current (dashed line) using chromium(III)hexacyanoferrate(II)modified BDD electrode.

4.2.2.3 Characteristic features of chromium (III) hexacyanoferrate (II) modified BDD electrode

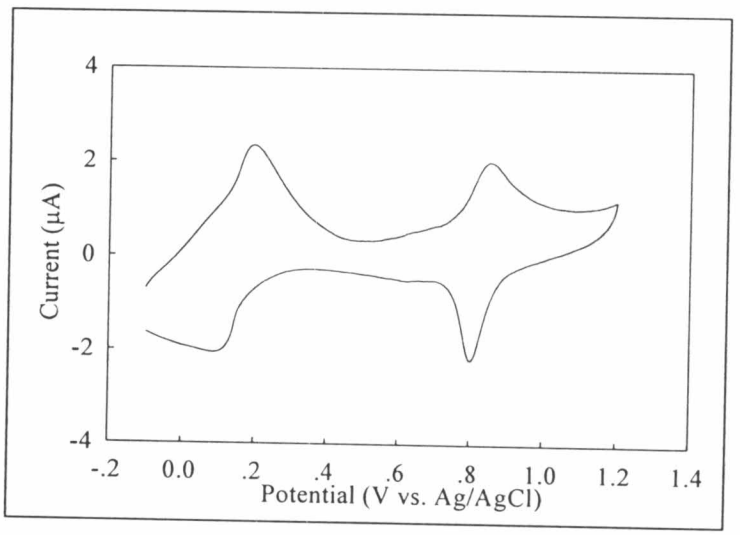

Figure 4.30 Cyclic voltammogram of 0.1 M potassium chloride (pH 3) at chromium (III) hexacyanoferrate (II) modified BDD electrode.

Fig. 4.30 shows the cyclic voltammogram of 0.1 M potassium chloride (pH 3) using chromium (III) hexacyanoferrate(II) modified BDD electrode. Two oxidative peak at around +0.20 and +0.90 V. vs. Ag/AgCl and the two reductive peaks are around +0.13 and 0.80 V. vs. Ag/AgCl were noticed., which are significantly different from the responses of the potassium hexacyanoferrate (III) or chromium (III) nitrate. These two peaks are attributed to different mixed-valence stages such as (2,2) to (2,3) or (3,2) to (3,3) indicated the formation of chromium (III) hexacyanoferrate (II) film on the surface of BDD electrode.

4.2.2.4 Voltammetric comparison of hydrogen peroxide using as-deposited BDD, anodized BDD, and chromium (III) hexacyanoferrate(II) modified BDD electrode.

The electrooxidation of 1 mM hydrogen peroxide in 0.1 M potassium chloride (pH 5) at chromium (III) hexacyanoferrate (II) modified was investigated. Comparison results were carried out using as-deposition and anodized BDD electrodes. The results were shown in Fig. 4.31. The ill-defined cyclic voltammogram were obtained using as-deposited and anodized BDD electrodes. On the other hands, well-defined cyclic voltammogram of hydrogen peroxide was

obtained from the electrocatalytic reaction of chromium (III) hexacyanoferrate (II) modified BDD electrode. The oxidation peak was observed at the potential about 0.8 V vs. Ag/AgCl. The electrocatalytic reaction of hydrogen peroxide by chromium (III) hexacyanoferrate (II) on the BDD surface was described as the following equation

Electrode reaction:

$K_2Cr(II)Fe(II)(CN)_6 \longleftrightarrow KCr(III)Fe(II)(CN)_6 + e^- + K^+$

Chemical reaction:

$KCr(III)Fe(II)(CN)_6 + K^+ + H_2O_2 \longleftrightarrow O_2 + 2H^+ + K_2Cr(II)Fe(II)(CN)_6 + e^-$

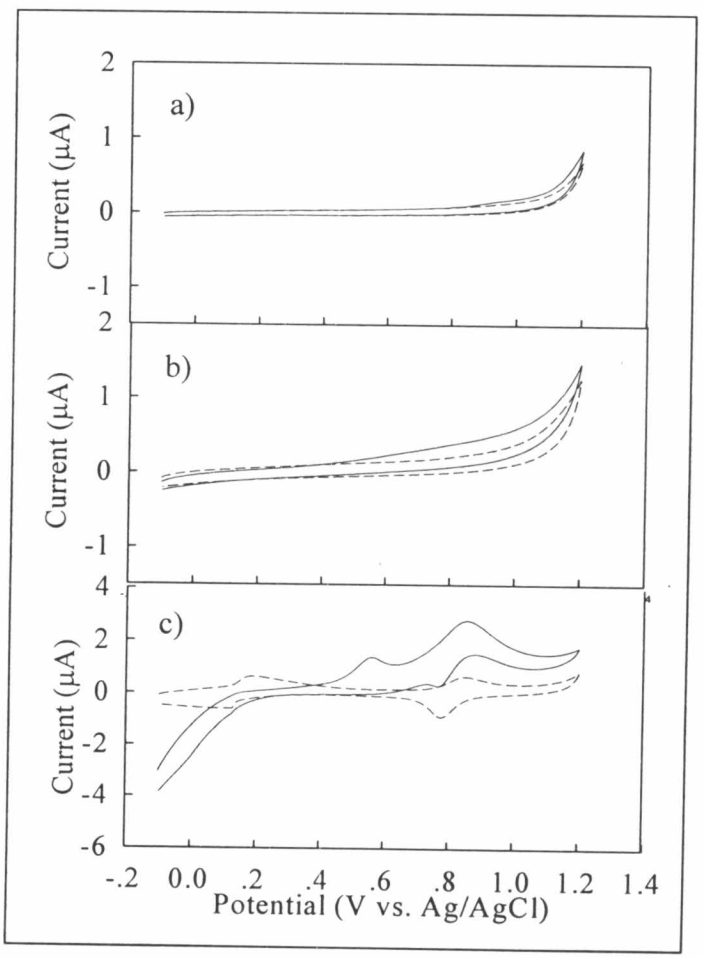

Figure 4.31 Cyclic voltammograms of 1 mM hydrogen peroxide (solid line) in potassium chloride (pH 5) together with the corresponding background current (dashed line) at a) as-deposited BDD electrode, b) anodized BDD electrode using 0.1 M sulfuric acid, and c) chromium (III) hexacyanoferrate (II) modified BDD electrode. The scan rate was 50 mV s^{-1}

4.2.3 Determination of hydrogen peroxide by flow injection coupled with amperometry

4.2.3.1 Hydrodynamic voltammetry

The detection potential of this modified electrode was evaluated using the hydrodynamic voltammetry. Hydrodynamic voltammogram was obtained from the average of three injections aliquot of the 20 μl of 100 μM hydrogen peroxide solutions by flow injection system. The applied potential value was increased at both anodic reaction from 0.3 to 0.9 V vs. Ag/AgCl (Fig 4.32a) and cathodic reaction from 0.1 to -0.7 V vs. Ag/AgCl (Fig. 4.28b). The carrier solution was 0.1 M potassium chloride (pH 5) (Fig 4.32b). From the results, we found that the optimum potential were 0.75 V vs. Ag/AgCl for the oxidation and -0.4 V vs. Ag/AgCl. The electrocatalytic reaction of hydrogen peroxide by chromium (III) hexacyanoferrate (II) on the BDD surface was described as the following equation:

Anodic reaction (oxidation reaction)

$$K_2Cr(II)Fe(II)(CN)_6 \longleftrightarrow KCr(III)Fe(II)(CN)_6 + e^- + K^+$$

$$KCr(III)Fe(II)(CN)_6 + K^+ + H_2O_2 \longleftrightarrow O_2 + 2H^+ + K_2Cr(II)Fe(II)(CN)_6 + e^-$$

Cathodic reaction (reduction reaction)

$$KCr(III)Fe(II)(CN)_6 + e^- + K^+ \longleftrightarrow K_2Cr(II)Fe(II)(CN)_6$$

$$2K_2Cr(II)Fe(II)(CN)_6 + H_2O_2 + 2H^+ \longleftrightarrow 2KCr(III)Fe(II)(CN)_6 + 2H_2O + 2K^+$$

However, the current response obtained from cathodic reaction was higher than the one obtained from anodic reaction. Moreover, the anodic reaction produced the oxygen gas that might be caused the irreproducible of the results. Hence, we used the potential at -0.4 V vs. Ag/AgCl to set the amperometric detector for the quantification experiments in flow injection system.

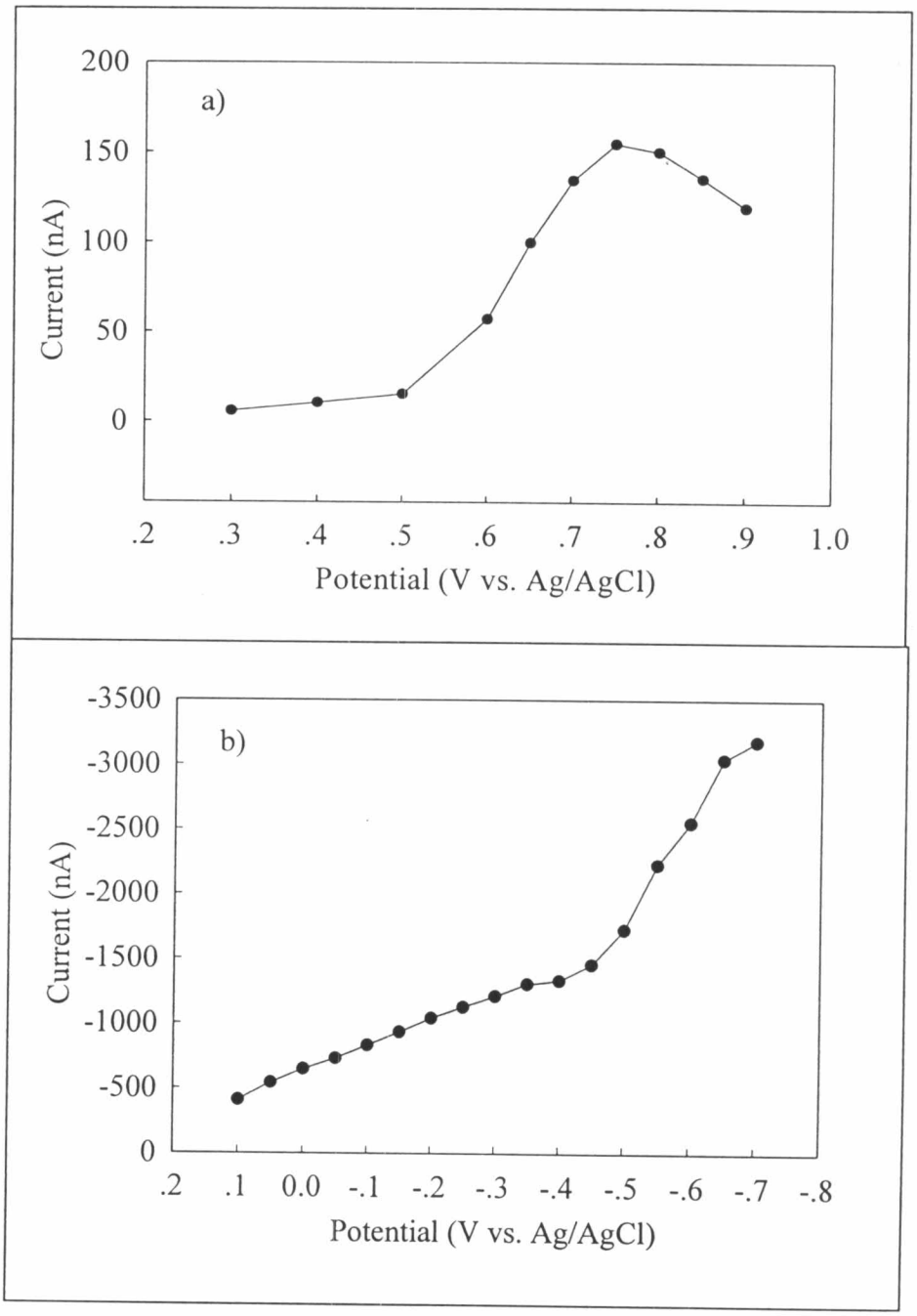

Figure 4.32 Hydrodynamic voltammograms of 100 μM hydrogen peroxide in 0.1 M potassium chloride (pH 5) a) anodic, and b) cathodic reactions.

4.2.3.2 Analytical performance of hydrogen peroxide determination at chromium (III) hexacyanoferrate (II) modified BDD electrode by flow injection system

A series of analytical figure of merit were performed on the proposed method for the quantification of hydrogen peroxide.

Linearity and LOD: Under the optimum conditions, the calibration curves were constructed in the concentration range of 0.088 to 4400 μM (Fig. 4.33). Each point of the calibration graph corresponded to the mean value from three replicated injections. The cathodic peak currents of hydrogen peroxide from 0.088 to 440 μM provided a linear line (i (nA) = -15.436 [hydrogen peroxide]-68.183 ; R^2 = 0.9981). The detection limit defined as the concentration providing the signal-to-noise ratio of 3 was as low as 0.044 μM.

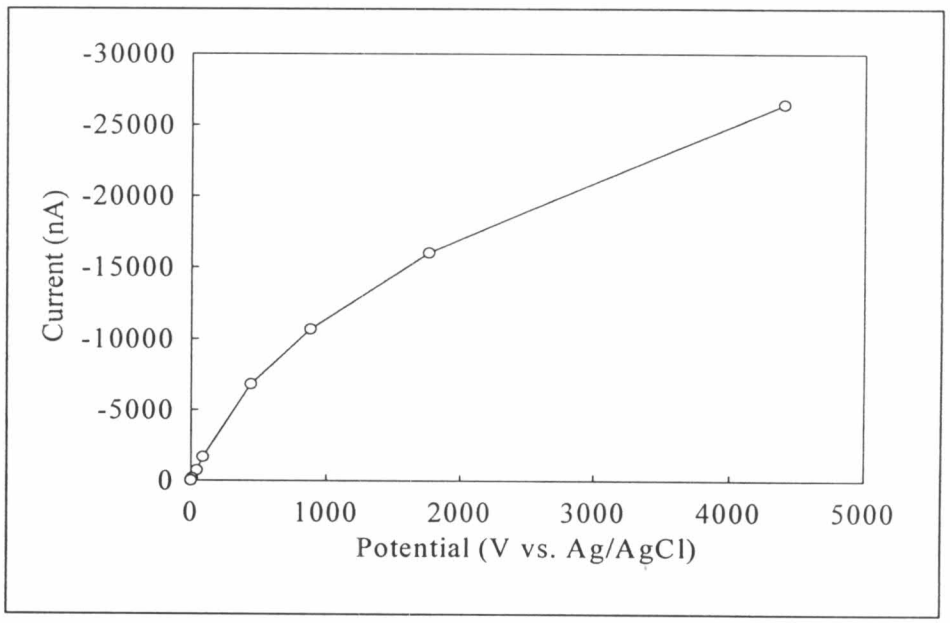

Figure 4.33 calibration curve of hydrogen peroxide standard solution in 0.1 M potassium chloride (pH 5).

Repeatability: To check the repeatability of the proposed method. The experiment was carried out by 10 successive injections of the 100 μM hydrogen peroxide standard solution (Fig. 4.34). The peak variability defined as the relative standard deviation (%RSD) was 1.0%.

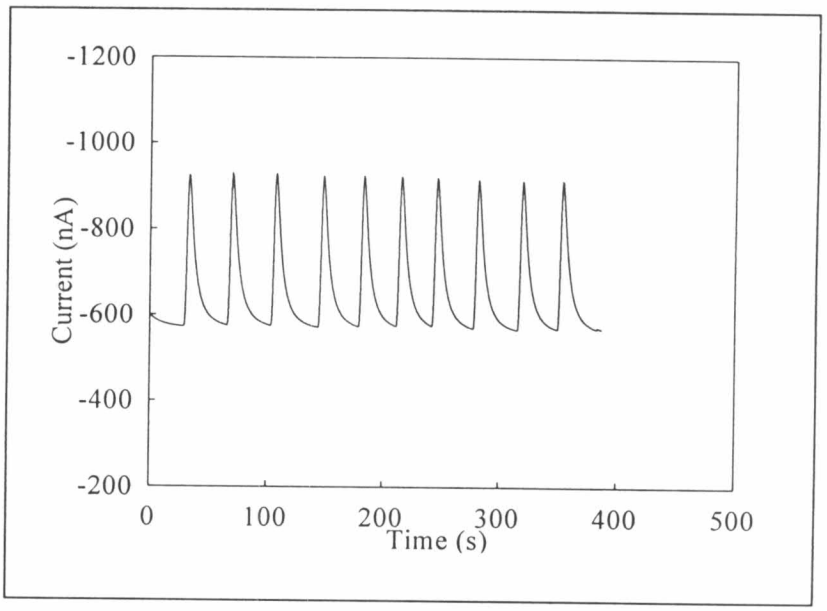

Figure 4.34 Flow injection with amperometric detection of 10 successive injections of 100 μM hydrogen peroxide in 0.1 M potassium chloride (pH 5).

4.2.3.3 Application of the proposed method.

Our proposed method was applied for disinfection solution using standard addition method. The precision of the method was based on the intra-assay. Figure 4.35 shows the standard addition graph of hydrogen peroxide. It was found that slope was -68.35 nA ml μg^{-1} and the intercept was -41.08 nA. The amounts of hydrogen peroxide obtained from the graph were compared to those labeled in the disinfection sample (3% w/v hydrogen peroxide). Relative errors compared with the claimed amount were lower than 5%. There was no significant difference between the labeled contents. To check the accuracy of the method, recoveries of the spiked standard solution were evaluated. The results were summarized in Table 4.17.

In order to verify the accuracy and precision of the proposed method, intra-day (n =2) recovery experiments with the standard addition method were carried out. The results of intra-day are summarized in Table 4.16. Recovery was also studied by addition of 4 standard concentrations (0.60, 0.9, 1.19 and 1.49 ($\mu g\ mL^{-1}$) to real samples. Recoveries obtained ranged from 98 - 105%.

The precision of the method was defined as the percent relative standard deviation. Three concentrations of added solution (0, 0.60 and 1.20 μg mL^{-1}) were chosen. Results obtained from 10 injections gave 2.0 - 2.4 % intra- assay studies, respectively.

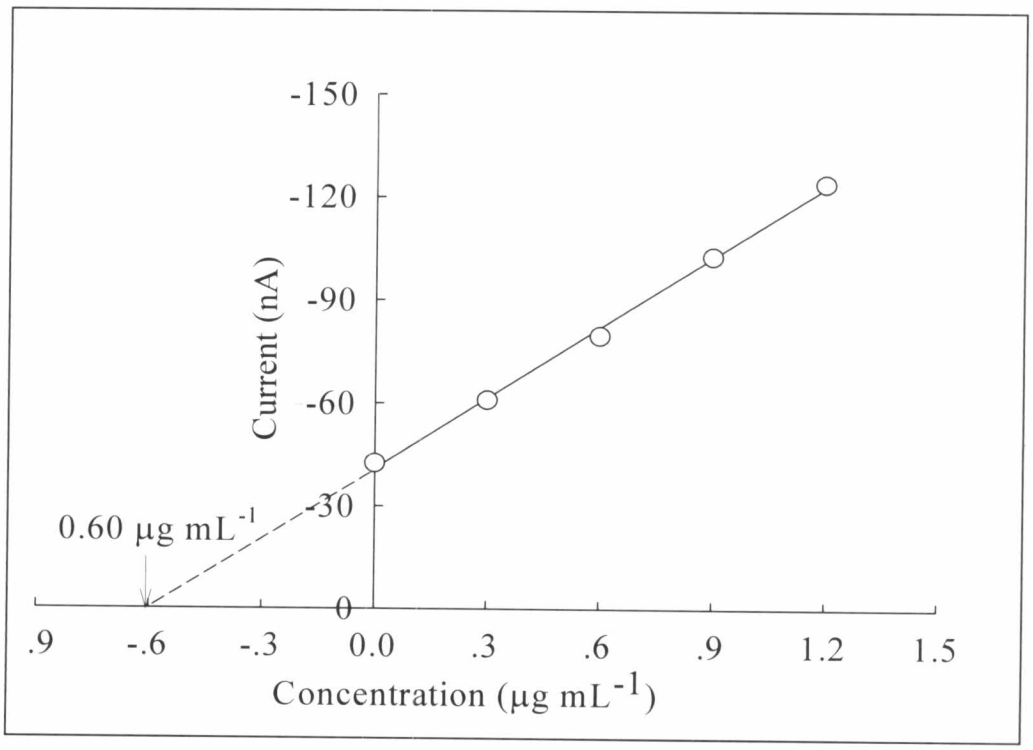

Figure 4.35 Standard addition graph of hydrogen peroxide sample.

Table 4.17 Recoveries of hydrogen peroxide disinfection sample with amperometric detection using chromium (III) hexacyanoferrate (II) modified BDD electrode applied to flow injection system.

Amount added (μg mL^{-1})	Intra-assay (n = 2)	
	Amount found (μg mL^{-1})	Percent of recovery (%)
0.30	0.29±0.00	96.8±0.6
0.60	0.59±0.04	98.9±6.6
0.90	0.91±0.01	100.8±0.6
1.20	1.19±0.03	99.5±2.2
3 % hydrogen peroxide	2.94±0.09	98.1±3.3